CAPTURE OF CIRCULATING TUMOR CELLS FROM BLOOD ON MODIFIED GOLD SURFACES INSIDE THE MICROFLUIDIC CHANNELS

A THESIS SUBMITTED TO
THE GRADUATE SCHOOL OF NATURAL AND APPLIED SCIENCES
OF
MIDDLE EAST TECHNICAL UNIVERSITY

BY

DIDEM ÇETIN

IN PARTIAL FULFILLMENT OF THE REQUIREMENTS
FOR
THE DEGREE OF MASTER OF SCIENCE
IN
BIOMEDICAL ENGINEERING

SEPTEMBER 2019

Approval of the thesis:

CAPTURE OF CIRCULATING TUMOR CELLS FROM BLOOD ON MODIFIED GOLD SURFACES INSIDE THE MICROFLUIDIC CHANNELS

submitted by **DIDEM ÇETIN** in partial fulfillment of the requirements for the degree of **Master of Science in Biomedical Engineering Department, Middle East Technical University** by,

Prof. Dr. Halil Kalıpçılar
Dean, Graduate School of **Natural and Applied Sciences** _____

Assoc. Prof. Dr. Ergin Tönük
Head of Department, **Biomedical Engineering** _____

Prof. Dr. Haluk Külah
Supervisor, **Biomedical Engineering, METU** _____

Assoc. Prof. Dr. Erhan Bat
Co-Supervisor, **Chemical Engineering, METU** _____

Examining Committee Members:

Prof. Dr. Tayfun Akın
Electrical and Electronics Engineering, METU _____

Prof. Dr. Haluk Külah
Biomedical Engineering, METU _____

Assoc. Prof. Dr. Erhan Bat
Chemical Engineering, METU _____

Prof. Dr. Uğur Tamer
Analytical Chemistry, Gazi University _____

Assoc. Prof. Dr. Selis Önel
Chemical Engineering, Hacettepe University _____

Date: 06.09.2019

I hereby declare that all information in this document has been obtained and presented in accordance with academic rules and ethical conduct. I also declare that, as required by these rules and conduct, I have fully cited and referenced all material and results that are not original to this work.

Name, Surname: Didem Çetin

Signature:

ABSTRACT

CAPTURE OF CIRCULATING TUMOR CELLS FROM BLOOD ON MODIFIED GOLD SURFACES INSIDE THE MICROFLUIDIC CHANNELS

Çetin, Didem
Master of Science, Biomedical Engineering
Supervisor: Prof. Dr. Haluk Külah
Co-Supervisor: Assoc. Prof. Dr. Erhan Bat

September 2019, 78 pages

Detection of circulating tumor cells (CTCs) from the bloodstream has a critical role in diagnosing and treatment of cancer. However, the number of CTCs in blood compared to other blood cells are extremely rare. In this thesis, various surface modifications strategies for detection of CTCs are studied in order to be used in the microfluidic detection systems. Functionalizing the gold surface with Self Assembled Monolayers (SAMs) used for attaching the EpCAM antibodies, which made possible to immobilize EpCAM protein expressing MCF-7 breast cancer cells. Cell binding events were monitored using fluorescent microscopy and antibody attachments through covalent binding and bioaffinity analyzed on different alkanethiol and polyethylene glycol (PEG) thiol SAM formations. The comparison between techniques was made considering the length and functional end of SAMs, homogeneous surface coverage, elimination of the nonspecific binding, positioning of the antibody and steric hindrance effect. Surface characterizations of SAMs and antibody attached surfaces were performed with X-ray Photoelectron Spectroscopy, Atomic Force Microscopy, and contact angle measurements. The selectivity to EpCAM protein was tested with K562 leukaemia cells. The experiments were repeated for other possible microfluidic surfaces, such as glass and polymer. Results

obtained from the comparisons are found useful for improvement on the antibody immobilization techniques for CTC capture on biosensor designs.

Keywords: Circulating Tumor Cells, Surface Modification, EpCAM Antibody, Gold Surface, Microfluidic Systems

ÖZ

KAN DOLAŞIMINDAKİ KANSER HÜCRELERİNİN MODİFİYE EDİLMİŞ MİKROAKIŞKAN KANALDAKİ ALTIN YÜZEY ÜZERİNDE YAKALANMASI

Çetin, Didem
Yüksek Lisans, Biyomedikal Mühendisliği
Tez Danışmanı: Prof. Dr. Haluk Külah
Ortak Tez Danışmanı: Doç. Dr. Erhan Bat

Eylül 2019, 78 sayfa

Dolaşımdaki tümör hücrelerinin (CTC'ler) kan dolaşımından tespiti, kanser teşhisinde ve tedavisinde kritik bir role sahiptir. Bununla birlikte, kandaki CTC sayısı diğer kan hücrelerine kıyasla oldukça nadirdir. Bu tezde, mikroakışkan algılama sistemlerinde kullanılmak üzere CTC'lerin tespiti için çeşitli yüzey modifikasyon stratejileri incelenmiştir. Altın yüzeyin, Kendiliğinden Oluşan Tekkatmanlı Yapılar (SAM'ler) ile işlevselleştirilmesi sayesinde EpCAM proteinini eksprese eden MCF-7 meme kanseri hücrelerinin EpCAM antikorları ile yüzeye bağlanması sağlanmıştır. Hücre bağlanma olayları, floresan mikroskobu ile farklı alkantiyol ve polietilen glikol (PEG) tiyol SAM oluşumları üzerinde analiz edilerek kovalent bağ ve biyo-afinite yoluyla bağlanan antikorlar kullanılarak analiz edildi. Teknikler arasındaki karşılaştırma, SAM'lerin uzunluğu ve fonksiyonel grubu, homojen yüzey kaplaması, spesifik olmayan bağlanmanın ortadan kaldırılması, antikorun konumlandırılması ve sterik engelleme etkisi göz önüne alınarak yapıldı. SAM'lerin ve antikor kaplı yüzeylerin yüzey karakterizasyonları, X-ışını Fotoelektron Spektroskopisi, Atomik Kuvvet Mikroskobu ve temas açısı ölçümleri ile yapıldı. EpCAM proteinine seçicilik K562 lösemi hücreleri ile test edildi. Deneyler, cam ve polimer gibi diğer olası mikroakışkan yüzeyler için tekrarlandı. Karşılaştırmalardan elde edilen sonuçların, biyosensör

tasarımlarında CTC yakalama için antikor immobilizasyon tekniklerinde gelişme için faydalı olduğu gözlemlenmiştir.

Anahtar Kelimeler: Dolaşımdaki Tümör Hücreleri, Yüzey Modifikasyonu, EpCAM Antikoru, Altın Yüzey, Mikroakışkan Sistemler

To mom,

It is my joy to be your daughter.

ACKNOWLEDGEMENTS

I would like to express my gratitude to my brother who always showing me the right thinking way in my worst circumstances with his sharp intellect and boosting self-reliance since my childhood, to my father for believing and trusting in me the things that I do not think I am capable of while waiting behind me as my wonderwall, and especially to my mother, for setting me free since my childhood to choose my way and while doing that for clearing all the rocks on that path. Also, as my second family, Başak Eren, Cansu Gülfidan, Gülce Başar and Melis Tanrıverdi, I am deeply grateful for finding you in the vastness of possibilities, because life is more tasteful when we share cooking recipes while we are far away from home.

My deepest gratitude in METU is to my supervisor Prof. Dr. Haluk Külah for his support and giving me the opportunity to involve in such a project. I would like to also thank Assoc. Prof. Erhan Bat for all the knowledge he shared with me.

For this thesis, BIOMEMS research group provided me lots of support and collaborations. I would like to thank my project partners Zeynep Çağlayan, Kaan Sel, Eren Aydın and Furkan Gökçe. Also, I especially want to thank Metin Dündar Özkan and Berat Yüksel for their contributions on my microfluidic chip production.

Last but not least, I am immensely thankful for meeting one of the cheerful person in our group, Meltem Okan Aydın. I will never forget how you stood by my side during my last year in METU. Without your push, this thesis and papers hardly would be realized.

Note: This work was supported by TUBITAK under grant number 213E024.

TABLE OF CONTENTS

LIST OF TABLES

TABLES

LIST OF FIGURES

FIGURES

CHAPTER 1

INTRODUCTION

1.1. Cancer Diagnosis

Cancer is the second leading cause of death worldwide and is responsible for 9.5 million deaths in 2018 [1]. In the future, the global burden is expected to increase further with the growing life expectancy, since it indicates that the cell has more time to accumulate mutations that develop through its lifespan. Cancer may occur when a cell in the body increases its number uncontrollably as a result of mutations in its gene. This is why no matter how the technology and our knowledge are massively increased; cancer still sounds scary for every person, and the complexity of evolution creates a huge challenge for the scientist to deal with.

Today, the global cancer diagnostic market size was valued at $144.4 billion in 2018 and it is expected to have $249+ billion in 2026 [2]. This growth is mainly caused by the increasing need for early diagnosis and the continuous introduction of innovative products to the market. Unfortunately, there is a significant number of people who cannot afford to undergo medical checks or the nearby health centers near them do not have specialized staff or equipment to perform such tests. Hence, governments and corporations are constantly striving for early diagnosis and the greatest advances are particularly made possible by the integration of the medical devices with the microelectronics. As a consequence, commercial implementations of microelectronic systems (MEMs) provided a wide range of research areas, particularly for the rare cell detection assays.

This thesis report discusses the common rare cancer cell detection systems that are used in MEMs devices and includes the application of antibody-based cell capture methods on the gold surfaces. The ultimate goal is to achieve the highest cancer cell

count by modifying the gold surface with self-assembled mono layers (SAMs) and employ cancer cell specific antibodies. This chapter summarizes the background information on cancer and the metastasis of it by the circulating tumor cells (CTCs). The detection strategies for these cells on microfluidic platforms are explained and important concepts are examined. Finally, the research objective and thesis organization are given.

1.1.1. Metastasis and the Importance of CTCs

The abnormal cell growth may form a mass called tumor almost anywhere throughout the body. If somehow these cells detach from their location in tumor and go to other places in the body through circulation, this tumor is called malignant (cancerous). Similarly, the tremendous increase in cell number could be malignant nevertheless, may not form a tumor tissue as in the case of leukemia, or there still could be an abnormal growth, but it considered as noncancerous (benign) if the cells do not have the ability to spread to surrounding tissues.

After the malignant primary tumor reaches a certain size, it begins to secrete chemicals in order to hijack the signals that stimulates vascularization through the tumor due to the need for oxygen and nutrients. Now that the tumor has been connected to a bloodstream, some cells that detach from the tumor generally spread to distant parts of the body with circulation system (Figure 1.1). In many cancer patients, it is certain that cells can spread from the primary tumor to the blood circulation, and that at least some of these travelling cells can form metastases [3]. It is estimated that 90% of cancer deaths are as a result of metastasis [4].

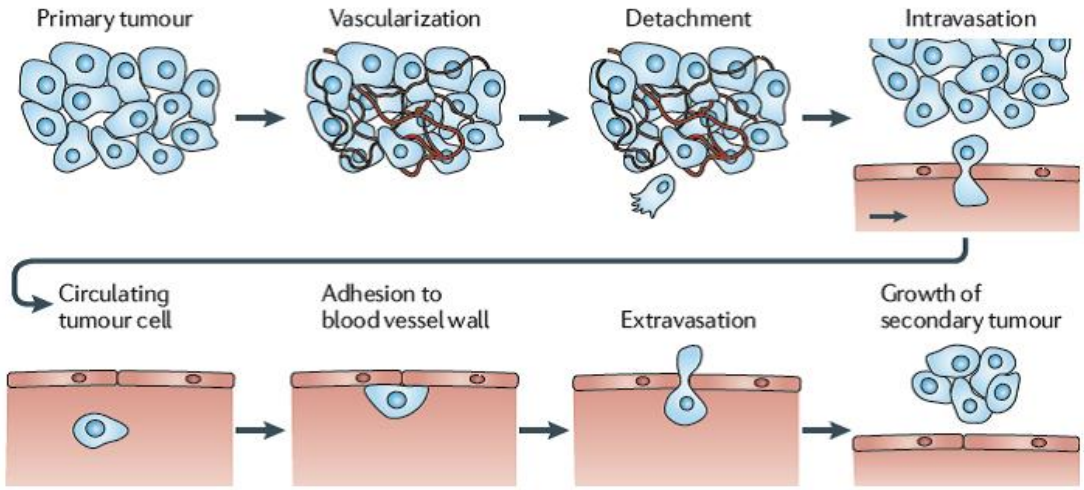

Figure 1.1 Metastasis process of cancer [5].

The biopsy is the most commonly used method for diagnosing cancer. It is done by taking a small sample from the primary tumor for a potential source of information. Treatment options can be decided by examination of the metastatic tissue sample [6]. But only one inspection of the metastatic lesion may not be sufficient to get a complete picture of the disease, because the genes and the microenvironment could change the tumor dynamics during the course of treatment and this brings patients to undergo lots of surgery [7,8]. As a result, inspecting the secreted materials from tumor in the circulation system has become an attractive option for doctors.

1.1.2. Liquid Biopsy

The identification and isolation of CTCs from circulation system, particularly in the early phases of the metastasis, may be crucial to decide on possible treatment options and monitor the patient's response throughout the treatment process. In addition to focusing on primary tumor site for genotype or phenotype changes to diagnose with a conventional biopsy, taking a blood sample can be easily done to achieve rapid information about potential molecular change throughout the treatment process.

Unfortunately, the downside of analyzing CTCs with the liquid biopsy is finding them within an excessive number of hematopoietic cells present in the blood sample. There are several million leukocytes and one billion red blood cells present in a ml of blood [9], whereas CTCs are present at the level of 1-10 cell in every 1 ml in metastatic cancer patients [10].

In addition to CTCs, liquid biopsy test on a sample of blood also includes fragments of DNA, tumor derived extracellular vesicles and exosomes from which apoptotic or necrotic cells released. In particular, the molecular profiling of the circulating tumor DNAs (ctDNAs) provides similar information and is present 100 times greater than CTCs. But they can be very short in length and specific primers need to be employed in PCR prior to analysis. These arrangements should be made immediately after the blood has been drawn from patient because the DNA fragments should not be circulating in the blood, so the half-lives of ctDNAs can range from 15 minutes to a few hours [11,12] and this degradation process may reduce sensitivity. Exosomes are another type of study, which carry a variety of molecules such as proteins, DNA or RNA for screening. However, the isolating them without any contamination by other exosomes in a limited life span is the major problem for their analysis [13,14].

The advantages of the cell capturing methods over nucleic acid methods include the potential to provide morphological identification and protein functional studies along with DNA analysis [15,16]. But distinguishing CTCs among numerous hematopoietic cells require extremely sensitive and specific isolation methods.

1.2. The Impact of Microfluidic Systems

Microfluidic flows are associated with dominant viscous drag forces (low Reynolds number) which lead to having laminar flow, because of the small channel dimensions. This laminar flow profile causes particles to go after streamlines and show tiny molecular diffusions across the channel, thus the molecules are transported in a relatively predictable manner. Also, the effect of surface tension and capillary forces

became much more important in microscale. Thus, precise and tunable flow properties for sample processing becomes easier to achieve.

Microfluidic systems have evolved greatly in recent years because of the technological developments in production and the increasing need for fast and efficient automated analytical platforms. Beyond the bench-top models, microfluidic devices aim to enhance the performance of the assay by minimizing the amount of costly reagents and samples while improving the sensitivity by eliminating human error. Also, microfluidic chips evolved from a single or multiple integration lab processes capable Lab-on-a-Chip Systems (LOC) to a micro total analysis system (μTAS) that capable of integrating more complex analysis systems for the immunoassay applications. Hence, these improvements have led to the development of point-of-care (POC) devices for rapid, accurate and low-cost biomedical analysis.

Over the years, microfluidic devices progressed from liquid handling to a single cell handling. Passive capillary force driven pregnancy and glucose tests evolved to an actively driven handheld i-STAT analyzers (Abbott Laboratories, Abbott Park, IL, USA) that can perform several blood tests. Later, the high throughput arrays allowed to perform millions of separate reactions in one experimental run, especially with the developments of droplet assays. The combination of droplet digital PCR with the integration of CTC isolation platform, CTC-iChip approach enabled CTC capturing [17].

In order to use microfluidic platforms in commercial applications in single cell analyses, microfluidics and μTAS systems should require microseparators, especially when working with the whole blood samples. Identification and separation of CTCs as a single cell without any clogging by eliminating the vast majority of the blood cells should be performed in high recovery and purity rates. Therefore, different capture strategies have been developed based on morphologic and chemical distinctions between CTCs and hematopoietic cells.

1.2.1. Label Free Isolation

Physical properties for instance size, deformability or electric charge are generally considered as label free isolations and using these properties allows the isolation of heterogeneous CTC capture without stressing the plasma membrane, which allows further downstream characterization.

1.2.1.1. Size Based Filtering

CTCs usually have a diameter of 15μm and larger than leukocytes of 8-11μm diameter and red blood cells of 5-9μm diameter [18]. This enables to use of porous commercial membranes for filtering the blood. Also, size determined filtering can be used by changing the rigidity of the wall so that the cell is forced to change its shape to pass a rigid gap and based on the deformability of the cells, a separation can be made [19]. However, microfiltration-based approaches could encounter clogging because of the bigger leukocytes and a large number of red blood cells, or any kind of cell cluster could limit the separation of CTC`s [20,21]. Morphological studies are showing that these cells phenotypically can be either round or oval and sizes can vary between 4μm and 30μm [10]. Also, subjecting CTCs to high mechanical stress could cause some changes in the identified CTCs [22].

1.2.1.2. Dielectrophoresis (DEP)

The cellular organization and the cell membrane of CTCs are usually different from the other hematopoietic cells based on their phenotypes and morphologies. This leads them to have certain dielectric properties and exhibit different polarizing forces under a non-uniform electric field. As a result, CTCs can be manipulated and separated from other cells with the dielectrophoresis (DEP) based methods [23]. There are several successful DEP applications for cell separation [24,25]. But unfortunately, the main disadvantage of DEP is that it offers low. In addition, cell dynamics could shift over

time due to ion leakage and the analysis must be performed in a short time. But, since the CTC recovery requires a large sample of volumes due to its rarity, the sensitivity and throughputs rates are decreased [26].

1.2.1.3. Hydrodynamic Focusing

Another idea for separation of cells using physical properties is to use hydrodynamic focusing in microchannels. Particles movement in flow results from the equilibrium of shear induced lift force and wall induced lift force. These two forces allow particles to migrate along the streamlines and can be expected within the channel for trapping based on the size of the particle (Figure 1.2).

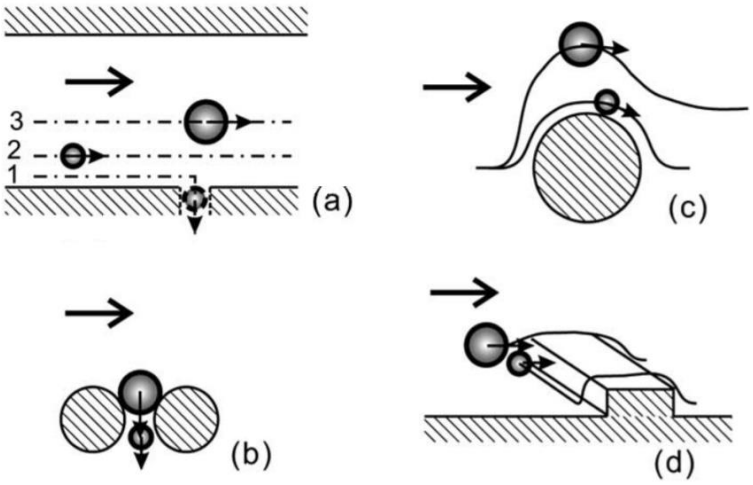

Figure 1.2 Cell motion in laminar continuous flow: (a) size determined distribution; (b) size determined filtering; (c) size determined displacement; and (d) size determined guiding [27].

This method can separate bigger cells from small ones but cannot be filtered out perfectly [27] and small Reynolds number in these systems can lower the throughput. To improve the efficiency, inertial microfluidics can be used to increase Reynolds

number to an intermediate region only by adjusting the flow velocity so that the particles can be focused on equilibrium positions on different cross section [28]. Besides the straight channels, in curved channels, secondary flow called Dean flow, pushes particles from the center which have a higher momentum than the inner wall to the outward channel due to the pressure gradient in a radial direction [29]. In these systems, it is crucial to determine the ideal flow rate and the channel length to achieve efficient separation. The advantage of this technique is the capability of large sample processing with a continuous operating mode which decreases the analysis time effectively. Also, the recovery of the tumor cell is very high, and cells are collected viable regardless of their heterogeneity.

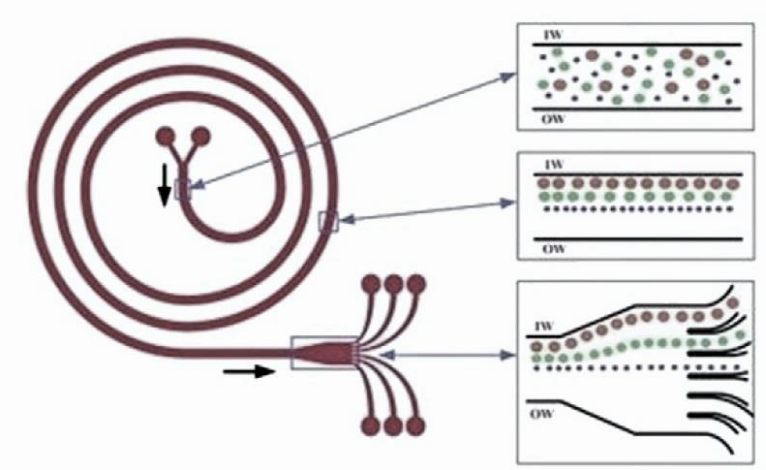

Figure 1.3 The location of the cells as they move through spiral microchannel [15].

On the contrary, some methods depend on breaking up these streamlines through microposts to create microvortices inside the channel. These methods generally used to enhance some cell interactions among the cell and the desired capture surface, which is very hard to achieve on continuous flow. One of the first successful applications of these approach was the CTC-Chip that has 78,000 antibody functionalized microposts to create passive blood in order to maximize collision [30]

Later, another alternative strategy was developed by the same group using herringbone grooves on the walls of the channel to disrupt streamlines [31] (Figure 1.4). The Herringbone-Chip (HB-Chip) design allowed higher throughput and increased CTC capture and it is one of the best examples that combine label free approaches with the affinity-based approaches.

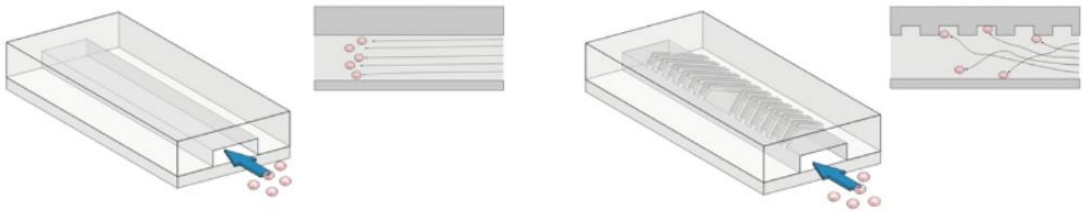

Figure 1.4 The laminar flow streamline disruption that herringbone design creates [31]

Label free methods made heterogeneity studies possible where lots of subgroups can be researched. It is particularly important for the CTCs that are highly heterogeneous and the ones that have gone to Epithelial to Mesenchymal Transition (EMT) by losing their epithelial expression markers, which expressed most of the epithelial origin CTCs (explained in detail in Section 1.2.2.2). However, it should be considered that CTC and leukocyte size overlap does not preclude the advances of unlabeled methods.

1.2.2. Affinity Based Isolations

The basic idea of affinity-based methods is to use the particular interactions among two molecules, for instance antigen and antibody or protein and nucleic acid. Such interactions could be covalent, ionic bonds and intermolecular bonds like dipole-dipole interactions and hydrogen bonds. Successful interactions require prior knowledge about the target molecule and the receptor. In this sense, CTC's cellular

membrane and the extracellular matrix researched deeply in order to differentiate it from the rest of the other cells through specific receptors, distinct signaling pathways or definite genetic materials. Cytometric and nucleic acid-based approaches focus on these alterations after the cell became CTC.

1.2.2.1. Nucleic Acid Based Approaches

Nucleic acid methods include isolating the ctDNAs in the circulation of a metastatic cancer patient as mentioned in Section 1.1.2 and capturing with the DNA or RNA aptamers, which are the single stranded nucleotides that can be identified by the cancer cells surface. Aptamers can be synthesized specifically for each subpopulation of CTC by SELEX (Systemic Evolution of Ligands by Exponential Enrichment) method and can easily be immobilized to a device surface. They can attach to their target with high affinity and form three dimensional structures. Although, there has been multiple successful applications on sensors and diagnostics [32,33], it has been much less efficient than expected and encounter with some problems [34,35]. The biggest handicap is the 2-minute degradation time, particularly on RNA aptamers, because of the nucleases in blood [36,37]. Different methods have been employed to increase the half-life of aptamers. One of the best-known applications is the Spiegelmers method that improve nuclease resistance to avoid quick aptamer degradation [38].

1.2.2.2. Cytometric Approaches

The main approach for the isolating the CTC is to use cytometric methods that are focused on the interaction of membrane antigens with the monoclonal antibodies. After the first monoclonal antibody production in 1975, their usage is bloomed and as of 2018, there are 80 FDA approved monoclonal antibodies on the market [39]. One of the most commonly used antigens for CTC capture is the epithelial cell adhesion molecule (EpCAM) because it is highly expressed in a variety of carcinomas such as

breast [40], lung [41], colon [42] and expression is restricted in normal epithelia cells [43]. As in the rest of the CAMs in normal tissues, it also mediates cell to cell adhesion and involves in processes like signaling, cell migration, proliferation, metabolism and differentiation [44]. An eye-catching study with EpCAM is done by The CellSearch® Platform which is the only device on the market that approved by the US Food and Drug Administration (FDA) in 2004. After coating magnetic beads with EpCAM antibodies, blood sample is delivered to EpCAM antibody covered ferrofluid nanoparticles and CTCs were selected as the blood passes through the magnetic field.

HB-Chip and CTC-Chip platforms choose to increase the collusion frequency of EpCAM antibody with the CTC to overcome the laminar flow profile as outlined in Section 1.2.1.3 and the incorporation of a microfluidic chip with the bioaffinity approaches allowed efficient CTC isolation from blood. CTC-Chip performed more than 60% lung cancer cell capture efficiency with the 50% purity rates and tested on 116 patient samples [30]. On the contrary to CTC-Chip, HB-Chip performed 92% prostate cancer cell capture yield and purity of %14 under 1.2ml/h flow rate [31]. When the flow rate increased to 4.8ml/h, the cell capture efficiency dropped only 8%. Likewise, the OncoBean Chip uses EpCAM antibody coated microposts for CTC capture inspired from the CTC-Chip, but under radial flow and achieve one of the highest flow rates in the market [45]. OncoBean Chip provides 10ml/h flow rate with more than 80% lung and breast cancer cells.

Detection of CTC is still difficult, because despite the high capture efficiencies achieved with the usage of EpCAM antibody, there is no marker that can reliably and selectively isolate the entire CTCs from the rest of the blood cells. Alternative prostate specific membrane antigen (PSMA) has been shown to capture of prostate cancer cells from blood [46] and geometrically enhanced differential immunocapture (GEDI) microfluidic chip system allowed high efficiency CTC capture from blood [47]. The system uses specially designed obstacles for size-based cell separation and the CTC directed into a PSMA antibody coated posts to increase the change of being captured

and provides 85% prostate cancer cell capture with a 68% purity rates under 1ml/h flow rate.

Epithelial cells typical characteristic tight junctions could be loss with the downregulation of the E-cadherin levels and cause cells to increase mobility. This epithelial phenotype loss is known as epithelial-mesenchymal transition (EMT) and normally happens during the embryonic development. Even though this process is complex and mostly unknown, there are researches focusing on isolating CTCs from the EMT markers such as Osteoblast(OB)-cadherin [48,49] (Osteoblasts are immature precursor cells responsible from producing many cell products for new bone matrix production and cadherins are the type of membrane protein that are gathered in adherent junctions and mediates adhesion between cells). OB-cadherin is mainly expressed in prostate cancer because it tends to metastasize to bone [50] and is relatively small amounts in breast [51], gastric [52] and bladder [53] cancers. The EMT process can serve as a secondary antibody after EpCAM and measurements can be made to observe E-cadherin levels.

Affinity based methods enables the identify CTCs regardless of the size variations and decreases the nonspecific cell capture with its targeted capturing. A certain type or combination of antibodies can be fixed to a desired surface and the identified cells can be isolated and analysed for further analysis.

1.3. Biomedical Applications Background

1.3.1. Cell Adhesion

Modifying the topographical properties of a surface to attach antibodies enables the CTC capturing in a microchannel. Understanding cell attachment plays a crucial role in microfluidic systems. Most mammalian cells are attached firmly to the substrate and as it sticks to the surface, the more it makes chemical bonds on its surface [54]. These attachments can be allowed to perform either in batch wise (static) or in

continuous flow (dynamic) in the channel. These adhesion bonds are formed by a transmembrane protein called integrins or with other adhesion molecules [55] (Figure 1.5).

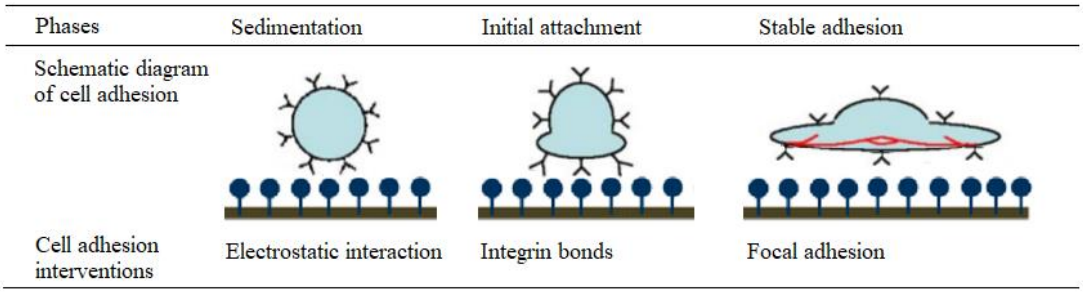

Figure 1.5 Static cell adhesion stages

In batch wise capturing, the sample is incubated for a certain period and then washed. The adhesion follows three steps, initial attachment to the substrate, flattening of the cell and finally fully spreading and structural organization [56]. Thus, as time increases, the adhesion becomes stronger.

On the contrary, in a continuous flow, adhesion cascade and signaling events become important and drive the tumor cell to make interaction with endothelium as in the potential metastasis (Figure 1.6). Adhesion cascade involves docking and locking phases. Docking process involves three steps, selectin mediated rolling which involves the initial recognition, followed by chemokine triggered activation that cause cells to roll slower and finally integrin dependent arrest. Locking phase starts after the stable bond formation with endothelial cells and continues very similar to the static adhesion [57,58]. To mimic this process in microfluidic systems, flow rates crucially important to achieve high throughput without compromising purity, recovery rate and viability. However, laminar streamlines in the microchannels inhibit the cell surface collusion and flow rates must be kept very small in order to allow cells to roll onto the surface on the channel to meet with its receptor. Unfortunately, achieving such small flow

rates almost impractical and that is why as mentioned in Section 1.2.1.3, passive mixing mechanisms are employed in microfluidic systems to disrupt the laminar flow.

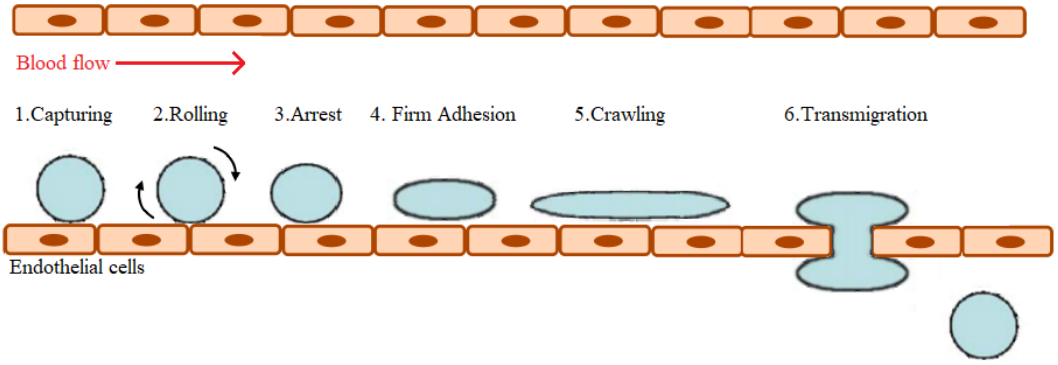

Figure 1.6 Dynamic cell adhesion stages

1.3.2. Surface Modification

The biosensor development and its performance strongly depend on the optimization of the surface functionalization. The surface of the sensor could be metal, polymer or glass. In order to construct a biorecognition site, the formation of Self Assembled Monolayers (SAMs), is one of the most preferred approaches in the literature [59,60]. Self-assembly creates ordered molecular structures that are formed spontaneously by the chemisorption of the head group with a specific affinity to a substrate (Figure 1.7). The linear hydrocarbon chain provides stabilization through van der Waals interactions and the terminal functional group of the molecule can be used to anchor different molecules either by weak interactions or by covalent bonds. In this respect, SAM based antibody incorporation allows oriented and direct anchoring on the surface than antibody physisorption [61].

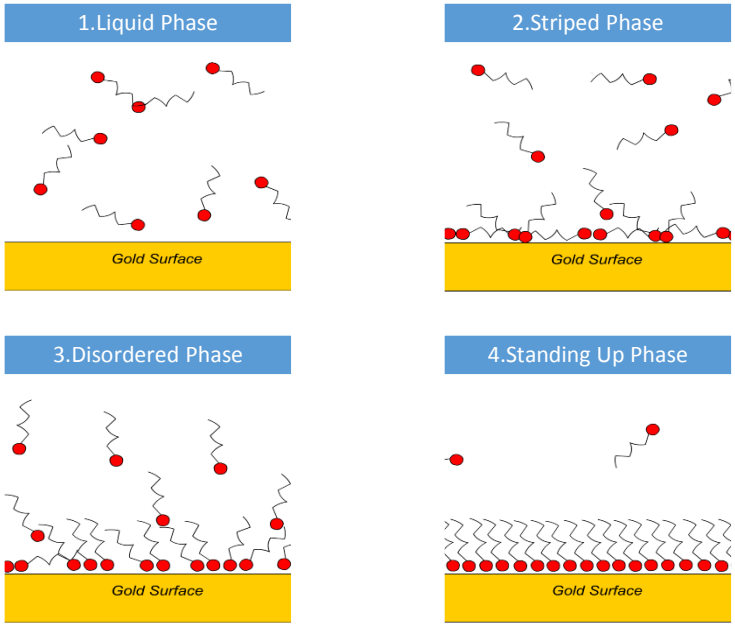

Figure 1.7 Alkanethiol formation phases [63]

Such SAM structure can be formed by thiols, silanes or phosphonates. But when gold surfaces are considered, SAMs that are based on gold-thiol interaction is highly preferable for allowing high affinity through the sulfur bond, decreasing nonspecific biomolecule adsorption and providing a robust biosensor surface [60,62].

1.3.3. Antibody Orientation

Generation of the interactions between the antibody and antigen on the surface of the biosensor depends on the number of receptors, binding affinity, bond formation rate. In order to achieve maximum efficiency, it is important to immobilize the antibody with specific orientations.

Antibodies are Y-shaped globular proteins which bind to specific antigens on the surface of a cell. Since there are vast amounts of different pathogens, antibodies are very versatile and very specific to their antigens. Antibody consists of two light chains

and two heavy chains with the integration of disulphide bonds at the hinge region. They also separated as fragment crystallizable region (Fc) and fragment antigen binding (Fab). Their orientation on the surface depends on the attachment of these two regions (Figure 1.8).

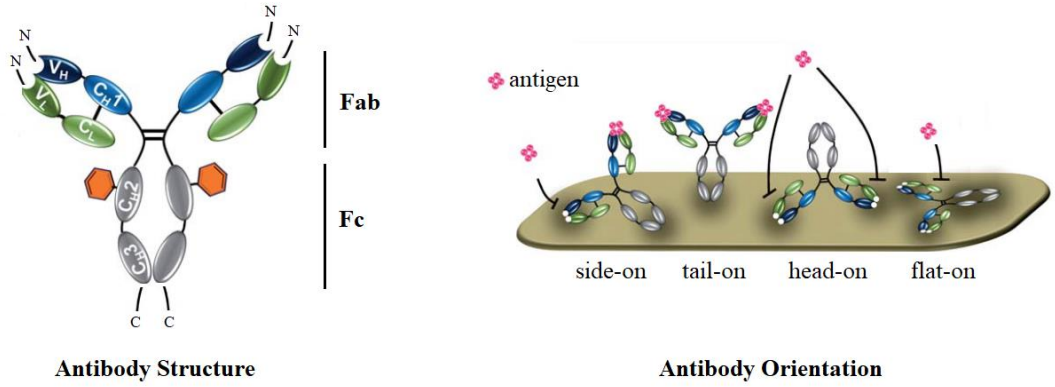

Figure 1.8 Antibody structure and possible orientations on the surface [61]

They bind to the pathogen to block their surface receptors and inhibit certain functions. These bindings are generally noncovalent interactions like hydrogen or van der Waals bonds [65].

When antibody and antigen come together, the long-range forces like hydrophobic interactions start to bring them closer and after coming nearby short-range interactions such as hydrogen bonds and van der walls starts to dominate. These interactions normally occur within the blood pH of 7.4 and for the microfluidic analysis, pH should be kept within the range of 6.5 and 8.5 [66].

1.3.4. Elimination of Nonspecific Bindings

When performing microfluidic studies, surface nontoxicity and inertness to different surface modification reagents or extreme pH values should be considered at the very beginning of the analysis. Also, since the overall aim of the microfluidic application is to make the analysis directly in the whole blood, any kind of contamination or nonspecific binding should be not allowed.

After coupling the antibodies, the target should bind to the desired areas of a bioreceptor with specific interactions, not to the rest of the surface. This could create damping effects or noise on the sensor. For this reason, blocking agents should have groups like hydroxyl or polyethylene oxide in order to prevent nonspecific bindings [67,68]. Bovine serum albumin used very highly in biology labs for eliminating the nonspecific bindings however, there is a potential of changing of its location with another suitable molecule, especially in the continuous flow microfluidic systems [69].

Polyethylene glycol (PEG) is one of the most popular water-soluble polymer used as surface modification agent that render surfaces biocompatible and also has the ability to present different functional groups at its terminal position which helps to control the structure. Protein repelling behaviour of PEG comes from the polymer backbone and its solvated configuration. Thermodynamically, the separation of water from the PEG chain is unfavourable and generates a steric repulsion which makes a contribution to the inertness of the PEG terminated surfaces [70]. This makes PEG suitable for microfluidic studies by offering suitable groups with its terminal end while rejecting protein binding to its long polymer backbone or by blocking the surface completely.

1.4. Research Objectives

The purpose of this study is to compare the antibody immobilization methods through different SAM molecules with respect to CTC capture efficiencies. Hence, surface modifications are aimed to be used in the CTC sensing application.

Considering the review, the objectives of this thesis can be listed as follows:

- Comparison of the effect of chain lengths using different alkanethiols and PEG thiols with respect to attachment of MCF-7 EpCAM positive breast cancer cell line model
- Investigation of covalent and bioaffinity antibody binding strategies through EDC: NHS coupling and streptavidin-biotin interaction
- Examination of the selectivity of modified surfaces using K562 leukemia cell line as EpCAM negative CTC model
- Examination of modified surfaces with blood
- Testing the modification methods with other possible microfluidic chip surfaces such as glass or parylene to observe specificity
- Characterization of surfaces after each modification step
- Implementation of the strategies to microfluidic channels

CHAPTER 2

MATERIALS AND METHODS

2.1. Materials

2.1.1. Gold Surfaces

MEMs based biorecognition devices take advantage of gold because of its nontoxicity and compatibility with other organic molecules. The combination of gold with sulfur containing linker used as the main strategy to attach antibodies in this study. Gold substrates are manually handled in each step of the experiment. These steps can be listed as follows:

1. Gold surface cleaning
2. SAM formation
3. Antibody conjugation
4. Cell capture analysis

To use in this study, bare gold surface and microfluidic gold channels were fabricated in METU MEMS Research and Application Center, Ankara, Turkey. Both CTC capture experiments and surface characterizations were carried out with gold surfaces (1cm x 1cm) coated on Si with 30nm thick and 300nm Au layers (Figure 2.1). For microfluidic channel tests, 650μm Si wafer coated with 500μm oxide, 20μm Ti and 200μm Au according to the gold channel patterned mask design. Previously fabricated SU-8 2075 spin coated over silicon wafer patterned with soft lithography and used as a master mold. PDMS poured over mold and cured at 70˚C for 2 hours and then peeled off. PDMS and oxide layer bonding performed with plasma oxidation at 15W for 20sec to achieve final microfluidic channel device (Figure 2.1, Figure 2.2).

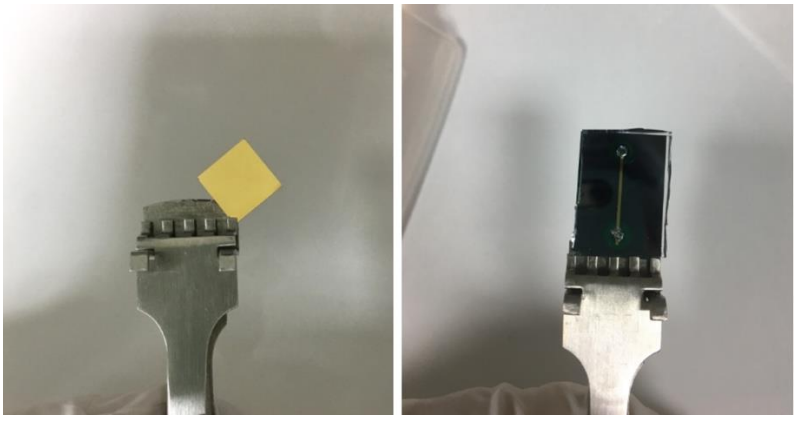

Figure 2.1 Modified surfaces, (left) bare gold surface, (right) PDMS microfluidic channel device

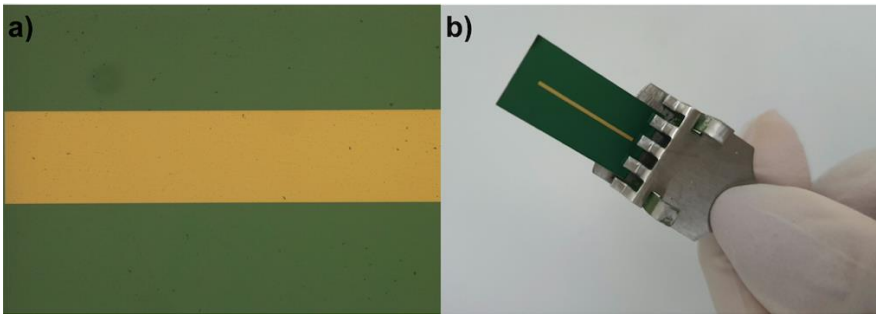

Figure 2.2 a) Microscope and b) real image of the chips used in microfluidic channel studies

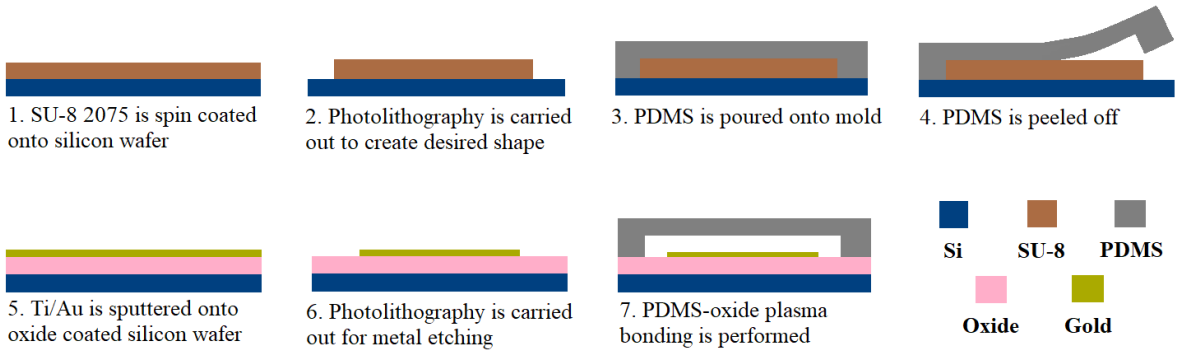

Figure 2.3 Fabrication flow of PDMS-oxide based channel device

2.1.2. Reagents

11-Mercaptoundecanoic acid (11-MUA) (%98), 11-Amino-1-undecanethiol hydrochloride (11-AUT) (99%), 4-Aminothiophenol (4-ATP) (97%), Cysteamine (Cys) (95%), 3-Mercaptopropionic acid (3-MPA) (≥99%), Poly(ethylene glycol) 2-mercaptoethly ether acetic acid(Mn2100), Poly(ethylene glycol) methyl ether thiol(Mn2000), Poly(ethylene glycol) amine thiol(Mn2000), N-(3-Dimethylaminopropyl)-N′-ethylcarbodiimide hydrochloride (EDC)(≥98.0%), N-Hydroxysuccinimide (NHS) (98%), Bovine Serum Albumin (BSA)(≥98%), Ethylenediamine (≥99%), Streptavidin from streptomycesavidinii, Phosphate buffered saline (PBS, 10× concentrate), MES monohydrate (≥%99,5), Fluorescein diacetate (FDA), were purchased from Sigma-Aldrich. The anti-EpCAM and Biotinylated anti-EpCAM were purchased from Abcam, UK.

2.2. Cell Model

For achieving the high expression level of EpCAM antigen, MCF-7 breast cancer cell line was used as the CTC model and cells taken from METU, Biology Department. As an EpCAM negative model, K562 leukaemia cell line was used. The cells used in the study were cultured on RPMI 1640 (Gibco) medium containing 10% fetal bovine serum (Capricorn) 1% penicillin / streptomycin (100X Capricorn) and 1% non-essential amino acid (100X Capricorn). The culture was maintained at 37°C in an incubator containing 95% humidity and 5% CO_2 until the cells were approximately 80% confluent. Cells reaching the fullness ratio were removed from the flask by a Trypsin-Edta solution (1X Capricorn). Cells taken as dissolved in 1ml RPMI 1640 were counted using Bio-Rad Tc20 Cell Counter and the total number of cells were determined. Cells were stained with fluorescence diacetate dye according to the manufacturer's instructions for fluorescence microscopy imaging. Washing was done by centrifugation at 300g for 7 minutes by removing the supernatant and dissolving in PBS repetitively three times.

2.3. Blood Studies

Blood samples were taken in tubes containing anticoagulant ethylenediamine tetra acetic acid (EDTA) from healthy donors as approved by the Institutional Review Board of METU Medical Center with the informed consent from all donors. Whole blood was immediately processed and lysed with red blood cell lysis solution (10x, MACS, Miltenyi Biotec.) according to the manufacturer's instructions. The remaining white blood cells were then precipitated by centrifugation with the same CTC preparation steps in order to be used in the experiments.

2.4. Surface Modification

2.4.1. Self-Assembled Monolayer (SAM) Formation on Gold Surfaces

All gold surfaces were first cleaned with piranha solution; a mixture of concentrated sulfuric acid (H2SO4) and 30% hydrogen peroxide (H2O2) (3:1, v/v). The surfaces were rinsed with deionized water, followed by ethanol and dried under nitrogen gas.

Once the surfaces were cleaned, they were soaked in freshly prepared alkanethiol solutions in ethanol at 5mM concentrations and incubated overnight (~16 h) at room temperature for SAM formation. For the PEG-thiol solutions, chloroform used to prepare 2mM concentrations and incubated overnight. Then, surfaces were rinsed with ethanol to remove feebly bound molecules.

The molecules used for SAM formation and their free functional groups are provided in Table 2.1.

Table 2.1 Thiol molecules and their structures

Terminal Functional End	**Structure**
Alkanethiols	
COOH	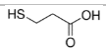
	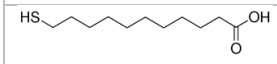
NH_2	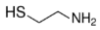
	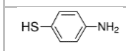
	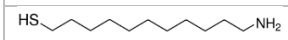
PEG Thiols	
CH_3	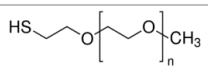
COOH	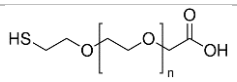
NH_2	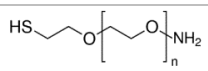

For the microfluidic studies, channel surface was cleaned with ethanol with 5.5ml/h flow rate and after being sure that there was no leakage in the channel, freshly prepared SAM solutions were sent to channel and incubated overnight under 0.5ml/h flow rate. Then surfaces washed with ethanol to remove unbounded molecules. Besides the cleaning process, all the channel experiment steps were performed under 0.5ml/h flow rate.

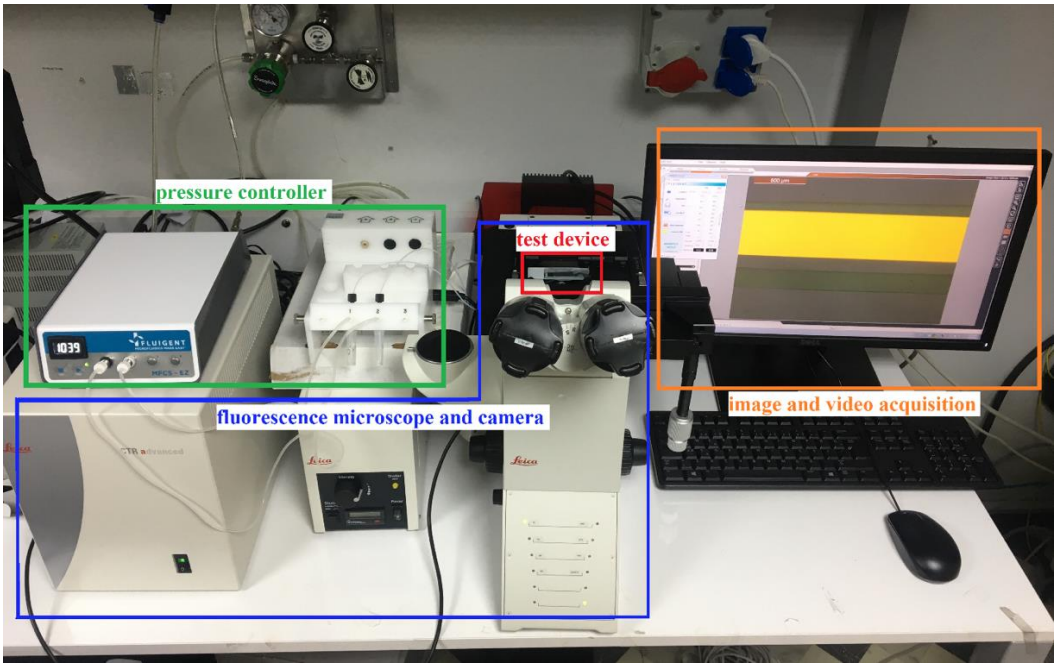

Figure 2.4 Test set up

2.4.2. Antibody Immobilization

Protocol 1. In order to activate carboxyl ended SAM surfaces, a solution of 10mM NHS and 10mM EDC were prepared in 0.1M MES buffer at pH5.0. Surfaces were incubated in this solution for 45 min at room temperature. Then the surfaces rinsed with PBS solution and incubated with 10 µg/ml anti-EpCAM antibodies in PBS for 2h at room temperature for covalent binding of anti-EpCAM antibodies onto the SAM modified surface. The gold surfaces then rinsed with PBS and incubated with 1% BSA for 15min at room temperature to block the free carboxyl ends without any antibodies attached.

Protocol 2. In order to activate carboxyl end of the antibodies, a solution of 10mM NHS and 10mM EDC were prepared in 0.1M MES Buffer at pH5.0 and mixed with 10 µg/ml anti-EpCAM antibodies in PBS solution (1:1, v/v). This solution was incubated for 45 min. Then, it was poured on the gold surfaces and immobilized 2h at room temperature for covalent binding of EpCAM antibodies onto the SAM modified

surface (Scheme 3). The gold surfaces were rinsed with PBS and incubated with 1% BSA for 15min at room temperature free amine ends without any antibodies attached.

Protocol 3. For the bioaffinity method, carboxyl ended SAM surfaces were activated with the solution of 10mM NHS and 10mM EDC prepared in 0.1M MES buffer at pH5.0. Then, the surfaces were treated with streptavidin solution (10 μg/ml) and incubated for 45 min at room temperature. Then, 10 μg/ml biotinylated EpCAM antibodies in PBS were incubated on the surface for 2h at room temperature. The gold surfaces were rinsed with PBS and incubated with 1% BSA for 15min at room temperature to block nonspecific sites.

2.4.3. CTC Capture

Once the antibodies were immobilized on the surfaces either through covalent binding or bioaffinity interaction, the CTC capture studies were performed. To image and track this process, a fully automated bright field microscope was used (Olympus SZX12, Olympus Inc.,) To be able to see the cells, they were previously treated with a fluorescent dye for 10 minutes. Capturing images of fluorescent signals emitted by fluorescent labelled cells immobilized on the surfaces was therefore made possible. The cells removed from the flask were prepared in RPMI 1640 and the total cell number was determined using the cell counter Bio-Rad TC20. The cells were precipitated by centrifugation three times by removing the supernatant and were suspended in PBS solution having a final concentration of 500,000 cells/ml.

Cell capture efficiencies were determined according to the analysis of the images taken at different positions of a surface by using Fiji Image J processing software.

2.5. Surface Characterization

2.5.1. X-Ray Photoelectron Spectroscopy (XPS)

XPS measurements were performed with PHI 5000 VersaProbe by Physical Electronics in METU Central LAB. Before taking XPS measurements, the surfaces were rinsed with PBS buffer and distilled water dried under nitrogen stream. AugerScan program was used for the calculation of relative atomic concentration by subtracted spectrum backgrounds with Shirley method. The neutral (C-C) carbon C1s peak at 284.6 eV was used as charge reference for XPS spectra.

2.5.2. Contact Angle Measurements

Surface contact angle measurements were taken for each of the functionalized surfaces with Attension Theta by Biolin Scientific in METU Central LAB. Surfaces were rinsed with PBS buffer and distilled water before the analysis and measurements were taken using sessile drop method. For each surface, contact angle was measured at five different locations and the arithmetic average was taken.

2.5.3. Atomic Force Microscopy

AFM characterization was performed to obtain information regarding the surface roughness and thickness after each of the functionalization steps. Images were taken with VeecoMultiMode V, from Veeco Instruments Inc., in METU Central LAB in dry state. Surfaces were rinsed with PBS buffer and distilled water and dried with nitrogen gas. The roughness and root mean square values were calculated using Gwyddion program.

CHAPTER 3

RESULTS

3.1. Fluorescence Microscopy Images of CTC Capture on Bare Gold Surfaces

This study focused on different alkanethiol and PEG-thiol usages for SAM formation on the bare gold surface and inside of the microfluidic gold channel in an external environment. Antibody exposure to the selected SAM formed surfaces was performed through carbodiimide crosslinking and the bioaffinity interaction using biotinylated antibody and streptavidin. Then, the antibody-SAM complex was used to detect CTCs in the sample solution.

Before channel tests and surface characterizations, optical imaging of gold surfaces was performed with a fluorescent microscope for each strategy in order to eliminate the surfaces that capture the lowest CTCs for further analysis.

3.1.1. Alkanethiol Studies

The experiments were carried out firstly with short 3-MPA and relatively long 11-MUA carboxyl end alkanethiols to determine the optimum length that gives maximum cell adhesion on surfaces, based on the several publications that use 3-MPA, 11-MUA or the mixture of them in gold channel designs [60,72-77]. Longer alkanethiols such as 16-mercaptohexadecanoic acid were previously recorded less efficient compared to 11-MUA [72] therefore, was not selected in this study. For the mixture of 3-MPA and 11-MUA, the 10:1 ratio have been reported the best molar ratio for achieving the optimum combination of reactive sites, as well as the steric hindrance of terminal groups [74,78] and used as the ratio for mixing two alkanethiols.

The incubation period of the alkanethiols was tested as 2, 7, 16, 24 and 48 hours but no significant difference was observed from the cell attachment assays after 16 hours. Different concentration values were tested to improve the accessibility of the thiol molecule because it is crucial to be more accessible for the antibody attachment. Concentration tests were also performed for EDC-NHS at different MES Buffer pH values, and optimum values were used in the experiments.

In Figure 3.1, cell attachment achieved with 3-MPA and 11-MUA and their carboxyl terminals allowed to immobilize antibodies on head-on positioning.

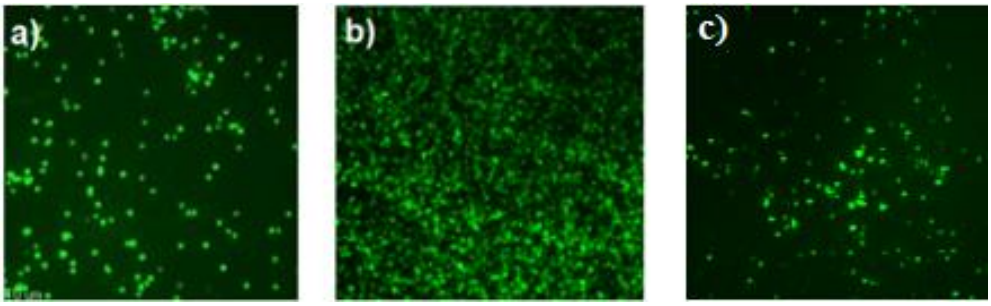

Figure 3.1 The Fluorescence microscopy images of attached CTCs on surfaces treated with a) 3-MPA b) 11-MUA and c)1:10 mixture of 3-MPA:11-MUA to create SAM

The images that were recorded in each experiment were analyzed using Fiji software program and captured cell numbers mean values calculated from 12 frames by repeating the same experiment three times and counting 4 different frames that belongs to one experiment. The results were found as 153±29 cell/frame for 3-MPA and as 1841±188 cell/frame for 11-MUA. Similarly, the 10:1 mixture of 3-MPA:11-MUA was performed very low CTC capture as 81±19cell/frame and it did not show consistent surface modification throughout the surface.

In order to test the amine functional ends on the SAM surface, Cys for its short length, 4-ATP to test a benzene ring and 11-AUT for checking against same length carboxyl

ended 11-MUA selected as amine terminated alkanethiols. In Figure 3.2 cell attachments to the tail on positioned antibodies can be seen on these alkanethiols modified surfaces.

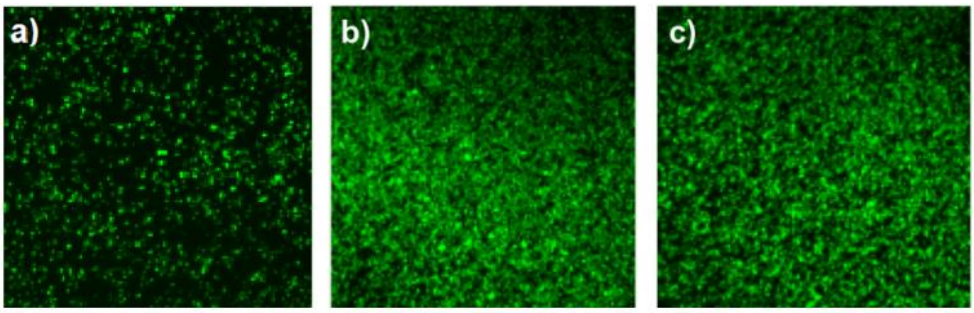

Figure 3.2 The fluorescence microscopy images of attached CTCs on surfaces treated with a)Cys b)4-ATP and c)11-AUT to create SAM

Analyzed images counted as 618±21.5 cell/frame for Cys, 1974±143.9 cell/frame for 4-ATP and 1937±257.4 cell/frame for 11-AUT modified surfaces. In each category, amine terminated SAMs were showing much better performance than carboxyl terminated SAMs. Similar to the 3-MPA, Cys resulted in less amount of cell attachment.

Up to now, all the antibody binding systems were covalently bonded to the SAM surface. An alternative strategy is to use bioaffinity since the affinity of streptavidin for biotin is known to be the strongest noncovalent biological interaction while promoting site directed antibody immobilization [85]. In Figure 3.3, surface coating with streptavidin on the 11-MUA was followed by the treatment with biotinylated EpCAM antibodies.

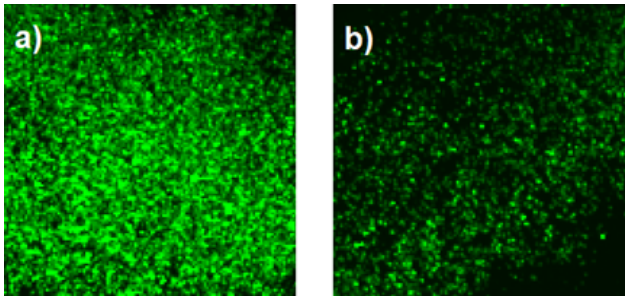

Figure 3.3 The fluorescence image of attached CTCs via streptavidin-biotin antibody onto a)2mM 11-MUA SAM modification b) 5mM 11-MUA SAM modification

When testing the bioaffinity methods to compare with the covalent method, different concentrations were again tested, and it was found that low concentrations SAM surfaces were providing more cell capture. The cell attachment on 2 mM 11-MUA was found as 1712±95 cell/frame. The overall cell capture amounts by different modified surfaces are provided in Figure 3.4.

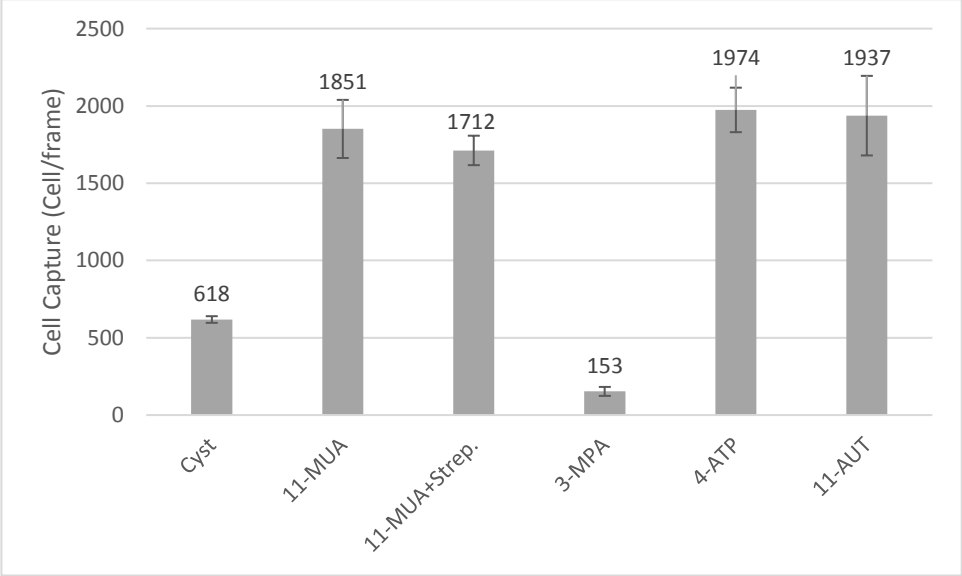

Figure 3.4 Cell capture efficiency comparison of the different alkanethiol formed SAM surfaces (cell/frame)

From this point on, the channel experiments and surface characterization continued using the alkanethiols that provided the most efficient CTC capture, namely 11-AUT, 11-MUA and 4-ATP. The short chain molecules Cys, 3-MPA and the mixture of 11-MUA with 3-MPA were eliminated because the cell attachment was not sufficient enough.

3.1.2. PEG-Thiol Studies

One of the downsides of using alkanethiol is the long formation time. So, rather than forming a brush like structures, using one of the most popular water-soluble polymer as a surface modification tool made possible to shorten the SAM formation time. Three different terminal end PEG-thiols used to test the CTC attachment and surface blockage. Figure 3.5 and Figure 3.6 shows the cell attachment after 16h vs. 3h PEG-thiol incubation.

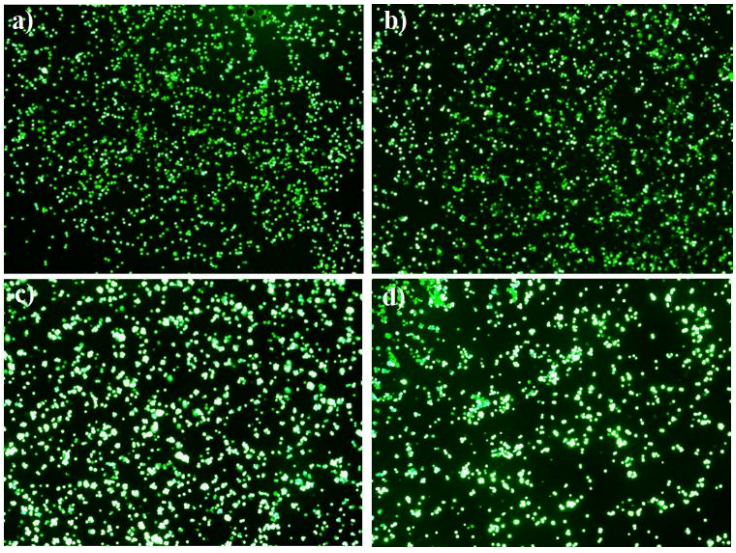

Figure 3.5 Fluorescence microscopy image of attached CTCs on the surfaces treated with 16h with a)PEG-NH_2 b)PEG-COOH and 3h with c)PEG-NH_2 d)PEG-COOH to create SAM

The cell attachment number were found as 904±291cells/frame for overnight PEG-NH_2 thiol incubated surface and 1272±180cells/frame for 3 hour incubated surface. The numbers for PEG-COOH thiol were counted as 818±60cells/frame for overnight incubated surface and 755±63cells/frame for 3 hour incubated surface (Figure 3.5).

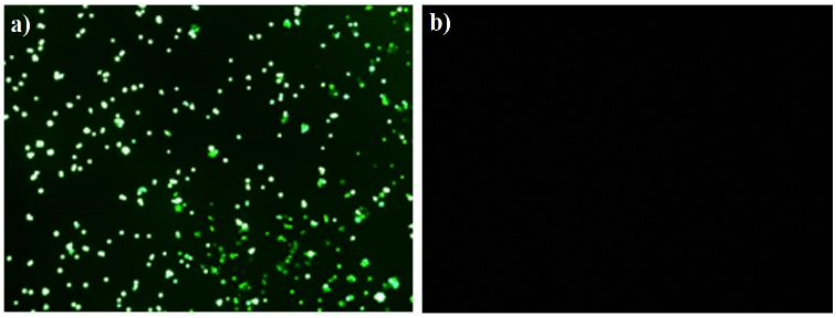

Figure 3.6 Fluorescent microscopy image of attached CTCs on the surfaces treated 16h with a)PEG-COOH:PEG-CH_3 mixture and b)PEG-CH_3 to create SAM

In order not to create a dense and crowded surface, surface manipulation trials were made with PEG-CH_3 thiol and its mixture with PEG-COOH with 10:1 ratio. As seen on Figure 3.6, PEG-CH_3 thiol created a total nonadhesive surface as expected with its methyl group and its mixture with PEG-COOH could be used for the desired surface attachment for CTCs.

In addition to the covalent binding systems, carboxyl ended PEG-thiol was used to test the bioaffinity method as an alternative strategy. Same as the other PEG-thiol surfaces, bioaffinity method tested overnight and 3-hour periods. The cell attachment found as 938±135cells/frame for overnightly incubated surface and 1261±141cells/frame for 3 hour incubated surface (Figure 3.7).

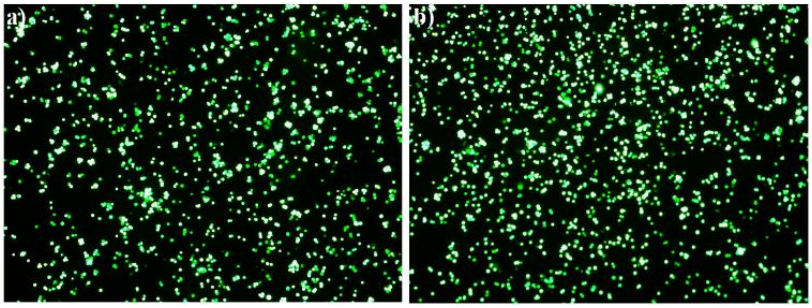

Figure 3.7 Fluorescence image of attached CTCs on the surface treated with a)16h PEG-COOH incubation and b)3h PEG-COOH incubation followed by streptavidin and biotinylated anti-EpCAM attachment

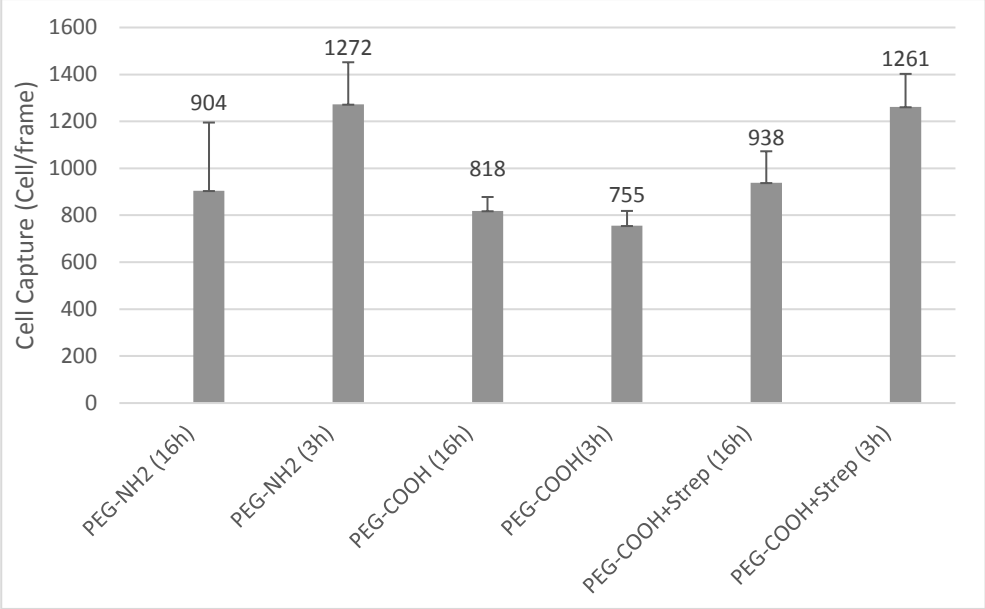

Figure 3.8 Cell capture efficiency comparison of the different alkanethiol formed SAM surfaces (cell/frame)

The high attachment rate on amine terminated PEG thiols were same as the amine terminated alkanethiols when compared to carboxyl terminated ones. The bioaffinity binding effects on the carboxyl terminated PEG thiols and alkanethiols were also found similar. But unlike alkanethiols, there is an unexpected increase with the 3-hour modified streptavidin covered PEG-COOH thiol surface.

3.1.3. Control Tests

Control tests were carried out using other possible microfluidic surfaces, such as parylene and glass to see whether SAM still forms and CTC capture works or not. The reason why parylene and glass were selected was that these are the most commonly used materials in many BioMEMS applications. All surfaces on Figure 3.9 were prepared following the same steps as done in the gold ones.

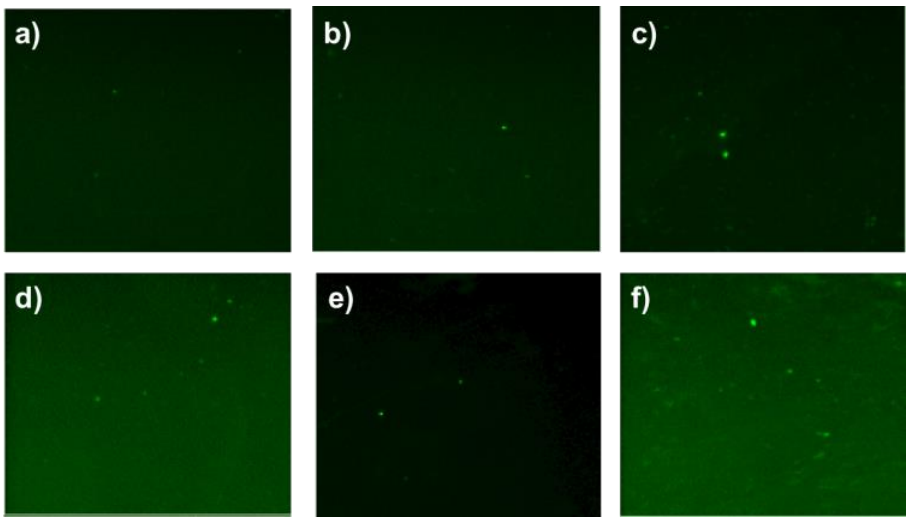

Figure 3.9 The fluorescent microscopy images of attached CTCs on parylene surfaces where SAM of a) 11-AUT, b) 11-MUA and c) 4-ATP were created and on glass surfaces where SAM of d) 11-AUT, e) 11-MUA and f) 4-ATP were created

As observed on Figure 3.9, there was almost no CTC capture by both surfaces, indicating that the SAM formation relies only on the gold-thiol interaction.

The further control experiment was carried out using a different type of cell, K562 leukemia cell, for which the EpCAM antibody should have no specificity. Gold surfaces again were prepared following the same steps with using 11-AUT, 11-MUA and 4-ATP alkanethiols. Figure 3.10 shows that K562 cells were almost not captured by the EpCAM antibodies.

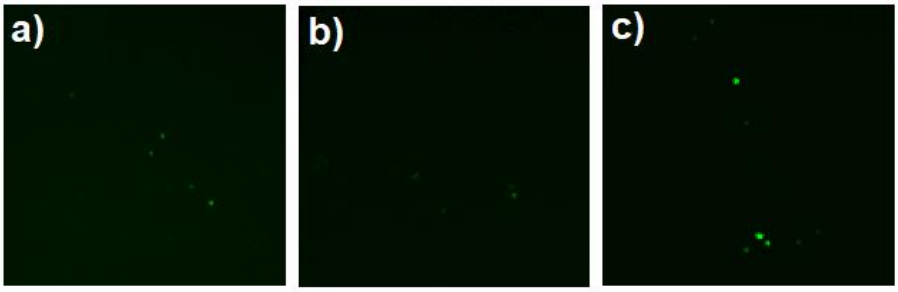

Figure 3.10 Fluorescent microscopy images of attached K562 leukemia cells on gold surfaces treated with a) 4-ATP b)11-MUA and c)11-AUT

For further cell capture studies on bare gold, real blood samples were used to see whether the system could work for the complex solutions. For this study, 11-MUA, 11-AUT and 4-ATP SAM surfaces were prepared and tested with the white blood cells remaining from the blood sample after the red blood cell lysis. The fluorescent microscopy images showed that there was no cell capture, indicating that the prepared surfaces worked fine (Figure 3.9).

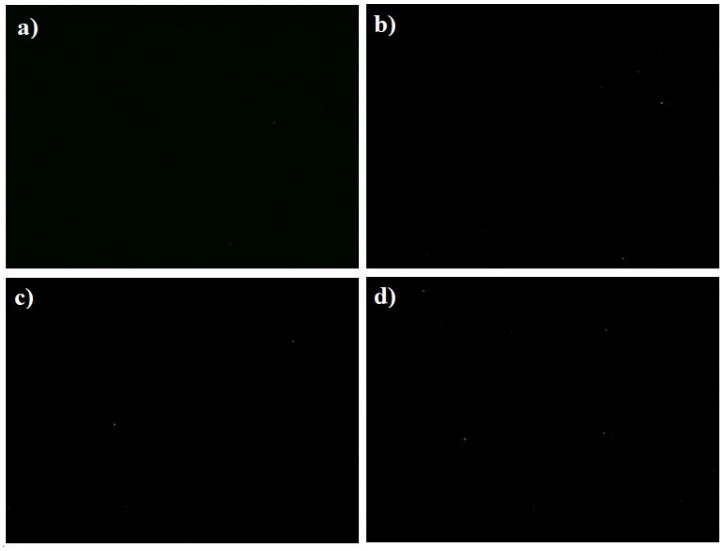

Figure 3.11 Fluorescence Microscopy image of the WBC attached to the a) 4-ATP b) 11-AUT c) 11-MUA d)biotinylated EPCAM modified 11-MUA surface

3.2. Microfluidic Channel Studies

Microfluidic studies started after the bare gold surface experiments and 11-MUA, 4-ATP, 11AUT, HS-PEG-COOH and HS-PEG-NH_2 selected for their CTC capture performances. Since the microfluidic chip did not have any channel design to minimize the CTC motion, the only possible way to allow CTC capture is to stop the flow in order to give the cells time to make an interaction with the antibodies. Once the cell solution started to enter the channel, the flow tried to be kept stationary as much as possible.

The cell solution is prepared as 200,000cell/ml for microfluidic channels to prevent cluster formation, but the number of cells enter the channel cannot be controlled manually. So, it should be noted that the cell capture efficiencies in channel experiments do not show the maximum possible cell capture efficiencies of the modified surfaces. The number of cells present in the microchannel was counted as N_i during the incubation period. Then the flow slowly increased to 0.10ml/h (6mbar) to remove unbounded cells and the remaining number was counted as N_0. The cell capture efficiency was measured as;

$$\text{Cell capture efficiency } \% = \frac{\text{The number of cells present in the channel after washing(No)}}{\text{The number of cells present in the channel during incubation(Ni)}} \times 100$$

3.2.1. Alkanethiol Studies

Before starting the 11-MUA modified and EpCAM antibody attached surfaces cell incubation period, the cell number entered to the frame counted as 104cell/frame. After the 10min incubation, the flow increased slowly to 0.10ml/h (6mbar) and cells did not change their location, besides one cell debris (Figure 3.12, marked as yellow). When the pressure increased to 0.34ml/h (20mbar), still none of the cells was detached. Even in some experiments, the flow increased to 0.51ml/h (30mbar) and no

detachment was observed. This shows how strong the covalent bonding between SAM and EpCAM antibody and the cell initiation to the surface.

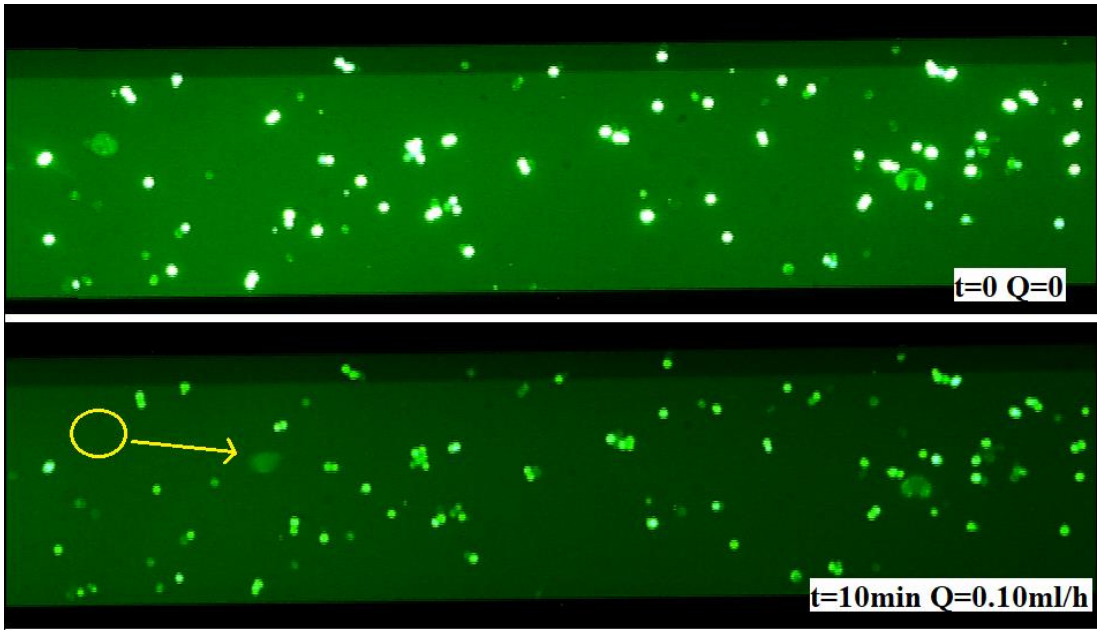

Figure 3.12 Fluorescence microscopy image of the attached CTC on 11-MUA modified EpCAM antibody covered surface

To compare the covalent bonding with bioaffinity interaction, 11-MUA modified surface covered with biotinylated EpCAM and the cells that entered the channel counted as 345cell/frame. After the 10 min incubation, the flow increased slowly to 0.10ml/h (6mbar) and cells were started detaching from the surface. In Figure 3.13, the detached cells counted as 13 cells/frame and this is equal to 96% capture efficiency in 0.10ml/h flow rate. When the flow increased to 0.34 ml/h (20mbar) the cells were detached more and the attached cell number decreased to 198cell/frame which shows

57% capture efficiency. This comparison showed that the CTC capture efficiency was significantly dropping when bioaffinity used in the channel experiments.

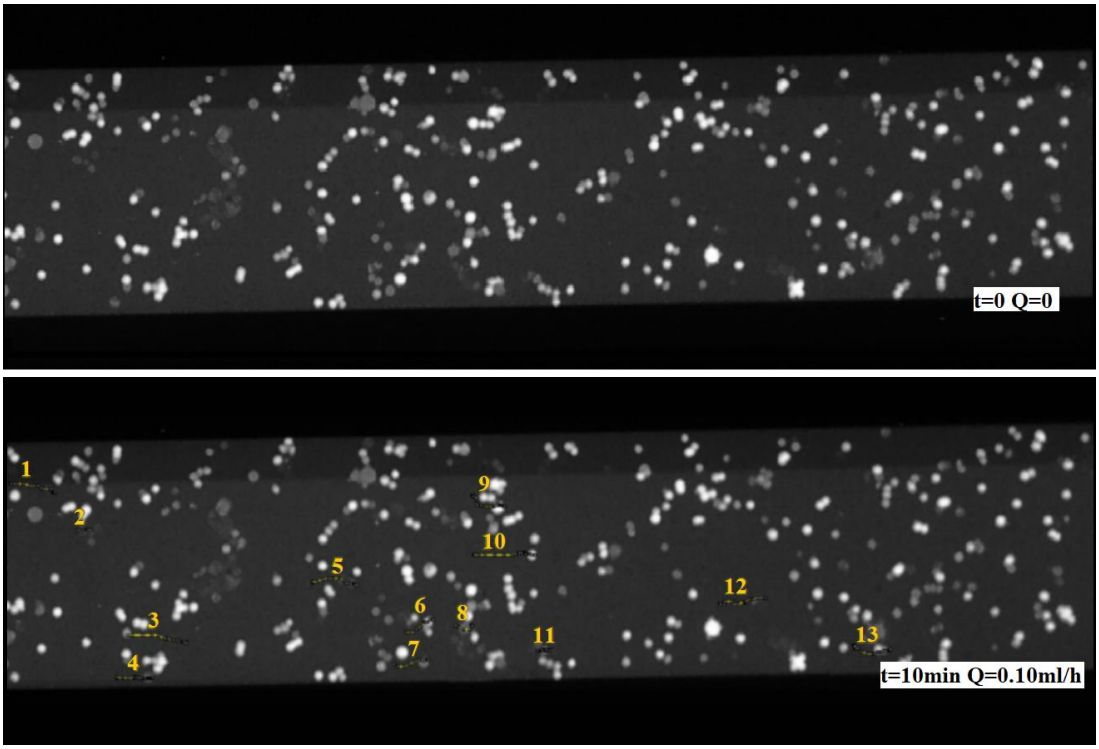

Figure 3.13 Fluorescence microscopy image of the captured CTCs on 11-MUA modified streptavidin-biotin EpCAM antibody immobilized surface

4-ATP was another covalently bonded antibody bounded but amine terminated surface that gave the maximum cell attachment on bare gold surface. In its channels experiment, stationary 75 cells are counted during the incubation phase. After the flow slowly increased to 0.10ml/h, two of the cells are detached from the surface (marked with yellow in Figure 3.11) When the flow increased further to 0.34ml/h, 73 cells were still on the surface beside traveling ones with flow and enter the frame during the picture was taken (Figure 3.12 marked as red), which means it kept its 97% cell capture efficiency.

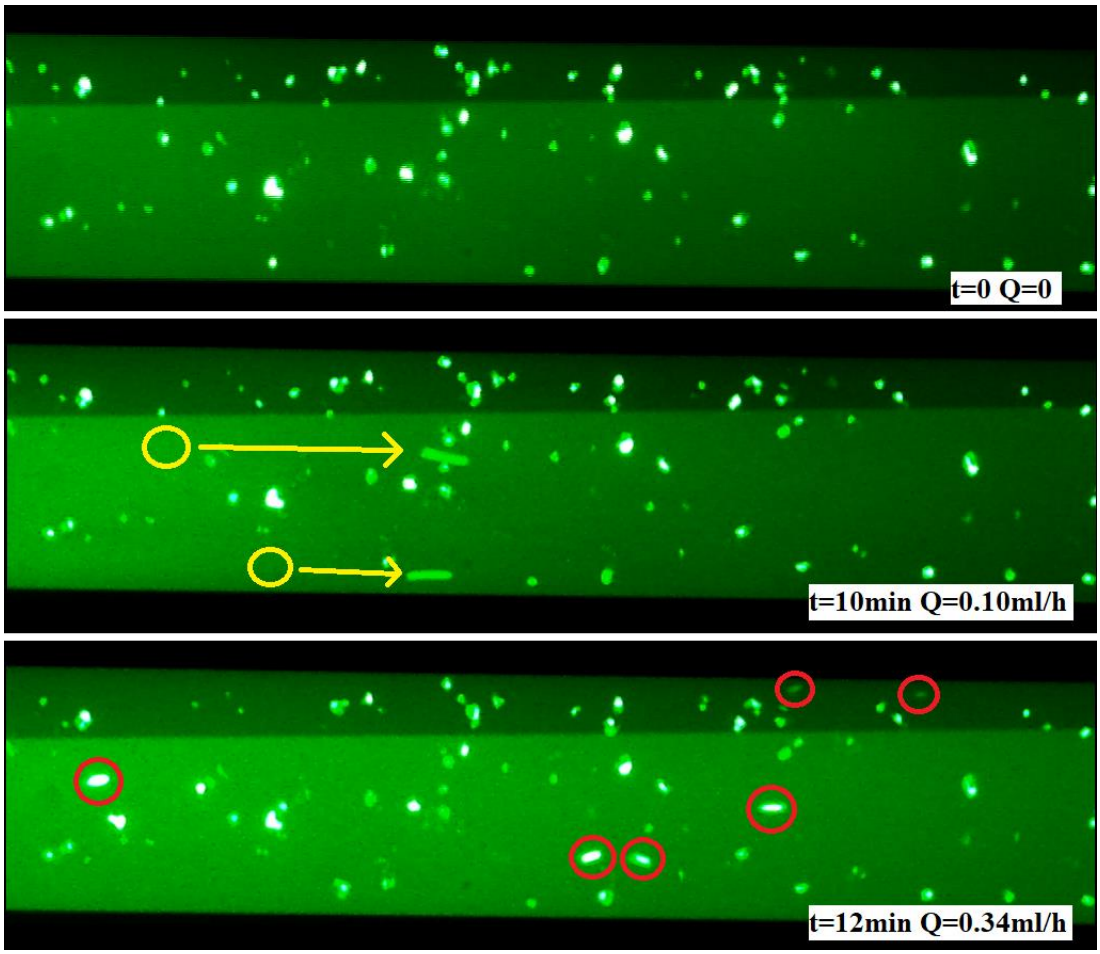

Figure 3.14 Fluorescent microscopy image of the 4-ATP modified surface yellow circles are the cells that were detached from the surface and the red circles are the cells that are traveling with flow and enter the frame

Another amine terminated surface was the 11-AUT. The counted cells before starting the incubation process was 43 cells/frame. After the 10 min incubation period, all the attached cells were still remaining even the flow rate increased to 0.34ml/h (Figure 3.15).

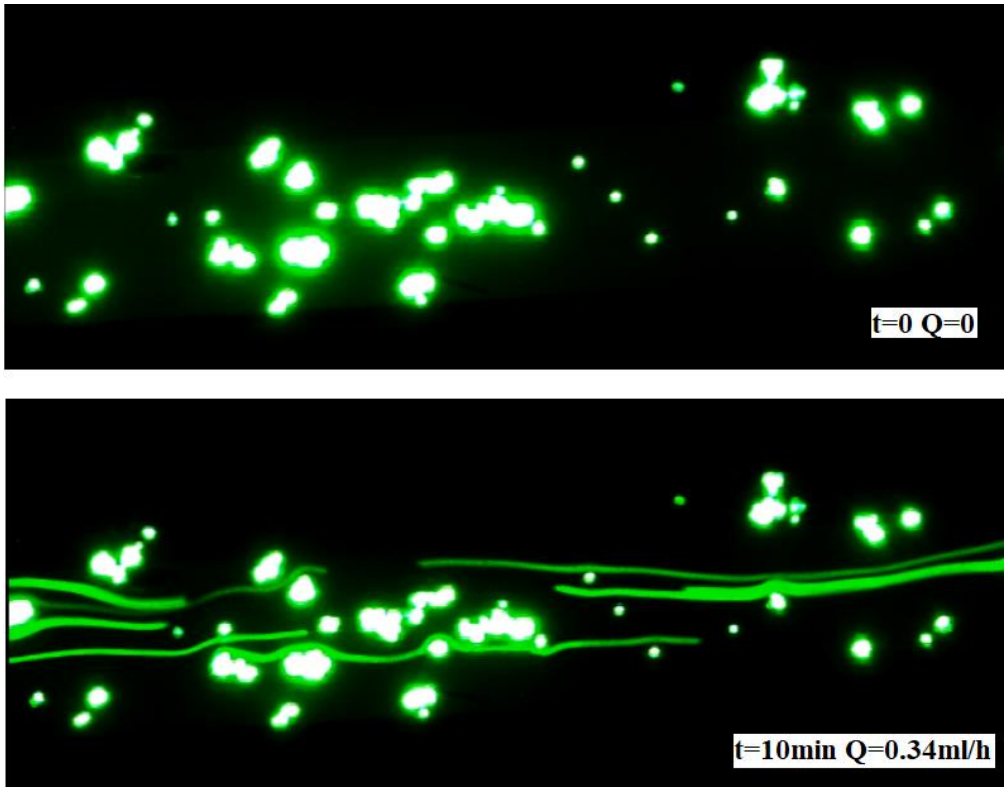

Figure 3.15 Fluorescent microscopy images of the 11-AUT modified channel surface.

3.2.2. PEG-Thiol Studies

For the PEG thiol channel experiments amine and carboxyl ended PEG thiols were used with overnight and 3-hour incubation periods. In carboxyl ended thiol surface, 20 cells were able to enter the frame and after 10 min incubation 20 cells were still remaining in 0.10ml/h flow rate.

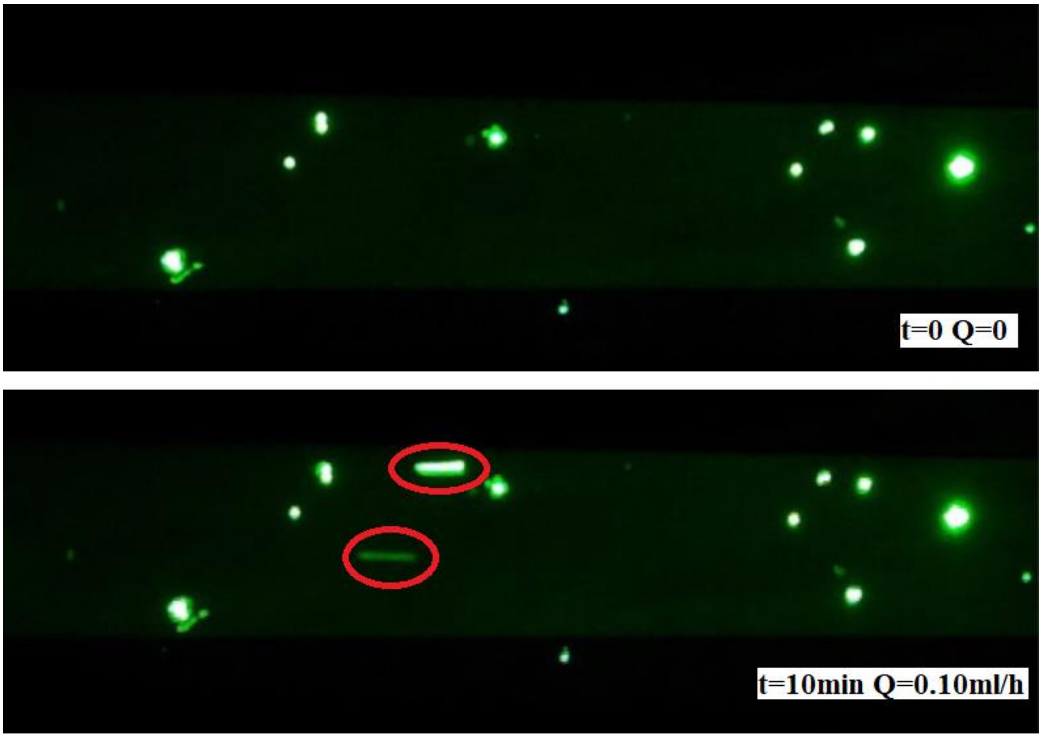

Figure 3.16 Fluorescent microscopy image of the overnight PEG-COOH thiol modified surface and the red circles are the cells that are traveling with flow and enter the frame

For the PEG-NH_2 thiol modified surface 3-hour incubation period tested and after the 10-minute incubation period, only 1 out of 47 cell was detached with the 0.34ml/h flow rate (Figure 3.17).

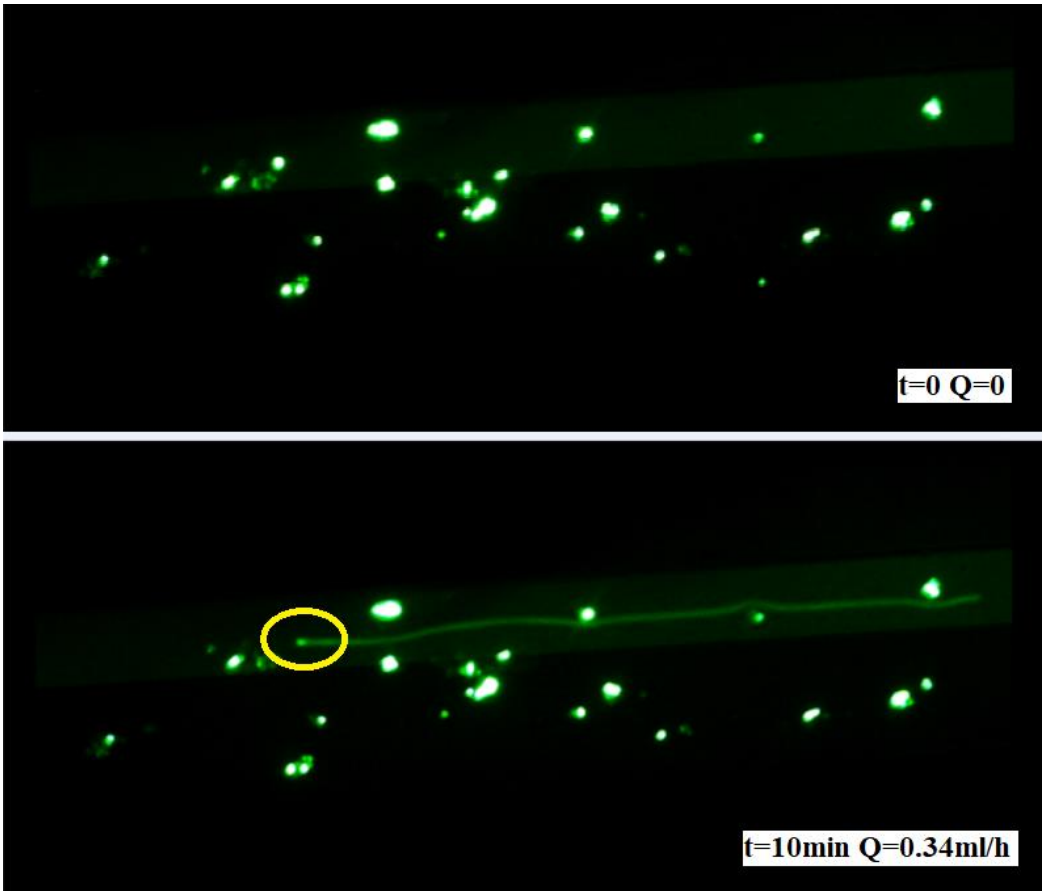

Figure 3.17 Fluorescent microscopy image of the 3hour PEG-NH_2 thiol modified surface yellow circles are the cells that are detached from the surface

To compare the bioaffinity method with covalent bonding, biotinylated EpCAM covered HS-PEG-COOH surface used in the channel experiment. Cells that entered to channel were counted as 33cell/frame before the incubation. When the flow increased to 0.10ml/h 3 of the cells were detached and after the flow reached 0.34ml/h, 2 more cells were detached. The 90% cell capture efficiency dropped to 84%.

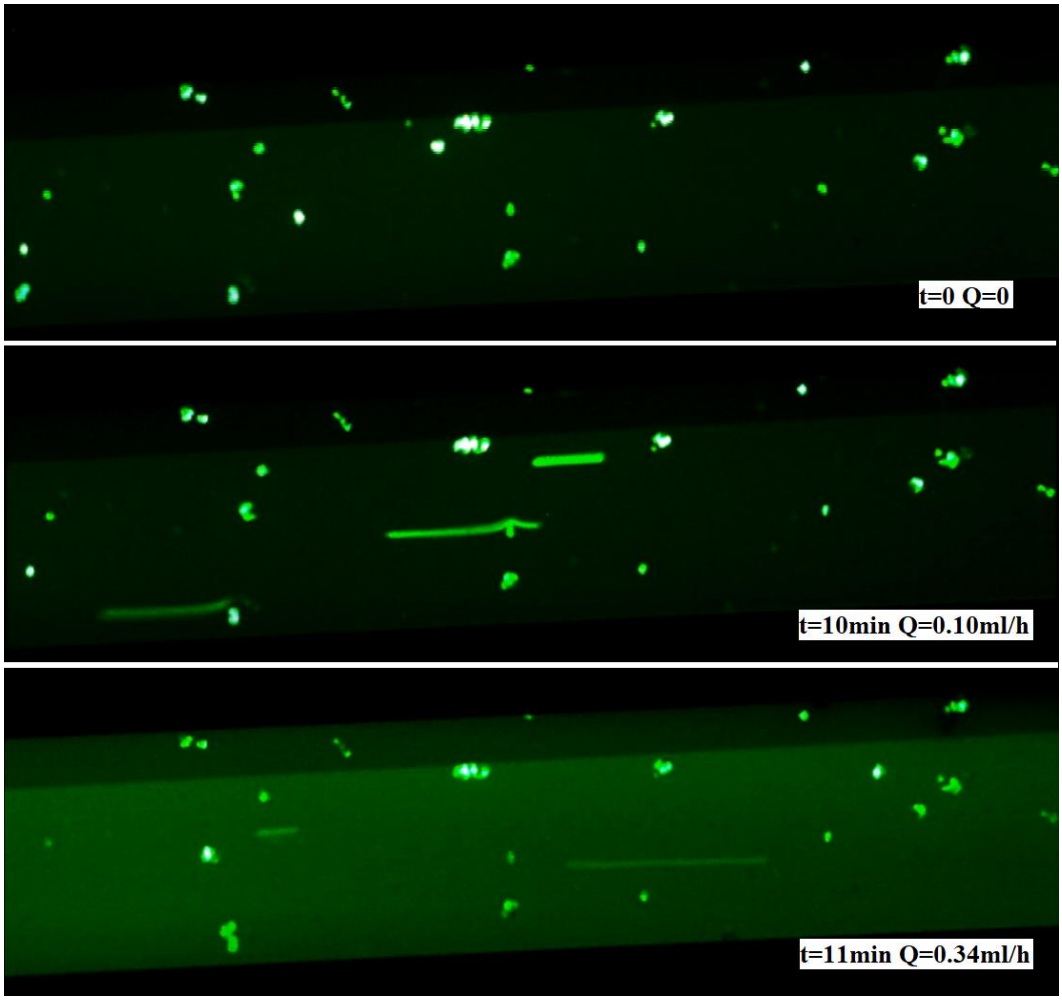

Figure 3.18 Fluorescence microscopy image of the PEG-COOH modified streptavidin-biotin EpCAM immobilized surface

Cell capture studies are performed in also dynamic flow conditions. Attempts to capture moving CTCs in high flow rates (0.34ml/h) were unsuccessful. But Figure 3.19 shows previously captured 3 and newly captured two cells at 0.05 ml/h flow. When the flow increased 10 times higher after 40 seconds, the location of one cell is changing while the location of the other cell is fixed. Since cellular adhesion are generally mediated by a small number of receptor ligand bonds, both the adhesion and detachment are a random variable.

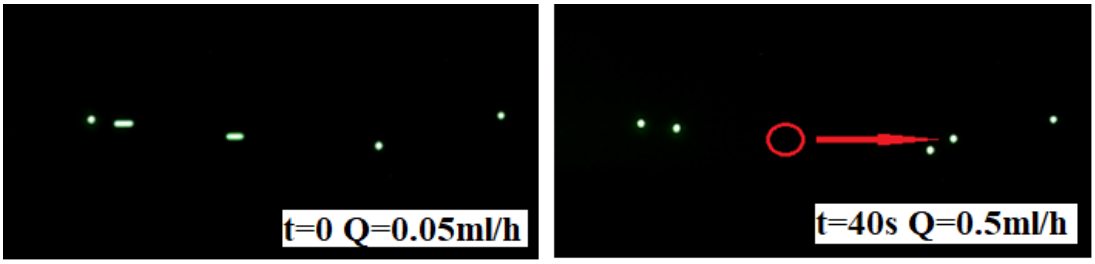

Figure 3.19 Fluorescence image of the cell capture on dynamic flow conditions on PEG-COOH thiol modified channel surface

In Figure 3.20, the total cell attachment number between t=0 and t=8min was 9 out of 10 cells with 0.05ml/h flow rate. And after this period even the flow rate increased further, none of the cells were detached. But, the downside of this dynamic flow method is the need for an excessive amount of time which leads to low throughput. Also, during period cells are starting to die in the channel after a while. This method could be efficient in gravity-based counting designs but not in a fluorescent image-based physical counting.

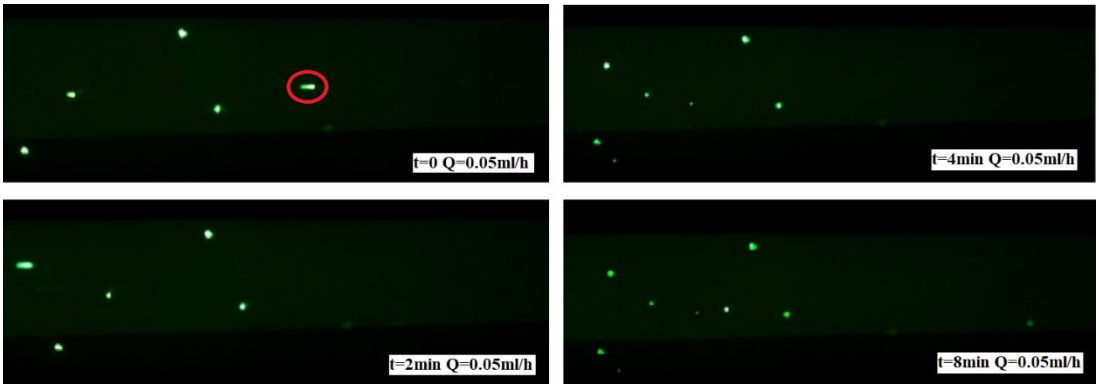

Figure 3.20 Fluorescence image of the cell capture on dynamic flow conditions on PEG-COOH thiol modified channel surface. The cell marked with red circle did not attached to the surface

Capture efficiencies of the modified surfaces are in Table 3.1. The covalently bonded surfaces were shown better performances than bioaffinity bonding of the EpCAM antibodies.

Table 3.1 Cell Capture Efficiencies of the Modified Surfaces

Cell Capture Efficiencies (%)	**0.10ml/h**	**0.34ml/h**
11-MUA	100	100
11-MUA+Strep	96	57
4-ATP	97	97
11-AUT	100	100
PEG-COOH	100	100
PEG-COOH+Strep.	90	84
PEG-NH2 (3h incubation)	100	97

3.3. Characterization of SAM formed Surfaces

3.3.1. Alkanethiol Studies

Atomic Force Microscopy (AFM) imaging was performed to visualize the surface topography of the SAM formed and antibody attached surfaces. The root mean square (RMS) roughness values were found to be 1.99±0.04 nm, 1.94±0.02 nm and 1.88±0.08 nm for SAMs created with 11-AUT, 11-MUA and 4-ATP, respectively. These RMS roughness values increased to 1.90±0.03 nm, 2.33±0.01 nm and 2.32±0.12 nm, respectively, after the antibodies were immobilized on the surfaces. For the bioaffinity method, 11-MUA-streptavidin covered, and biotinylated antibody covered surfaces RMS value found as 2.04±0.03 nm. and This increase ensures that antibodies were successfully bound to the free ends of alkanethiols.

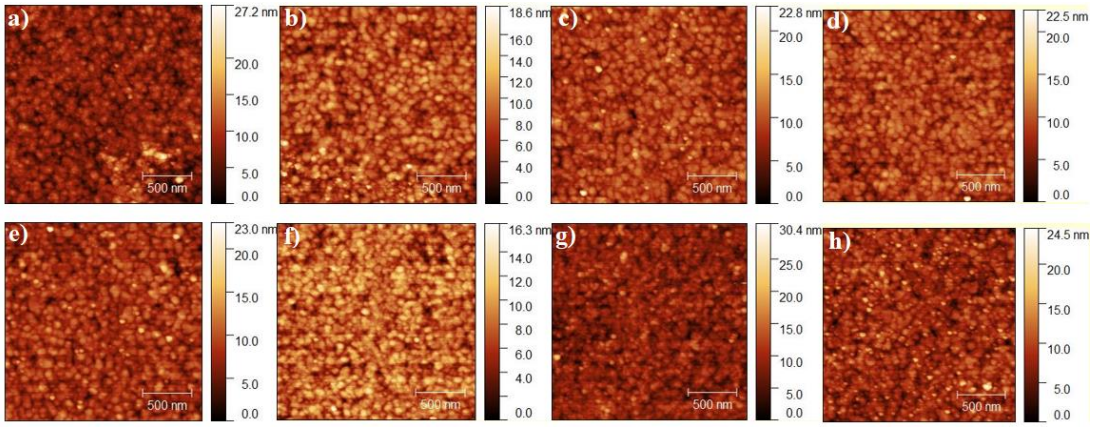

Figure 3.21 AFM images of a) bare gold surface, SAM formed with b) 11-AUT, c) 11-MUA, d) 4-ATP biotinylated antibodies immobilized on surfaces with e)11-MUA and antibodies immobilized covalently on surfaces with f) 11-AUT, g) 11-MUA and h) 4-ATP.

EpCAM antibody attached aromatic ring (4-ATP) causes more RMS roughness than other linear alkanethiols because of its nonlinear SAM structure. The structural difference between 11-AUT and 11-MUA can lead to distinctive results since the presence of amine functional group influences the SAM due to the hydrogen bonding between amino groups [88].

To investigate the elemental composition of each surface modification strategy, X-RAY Photoelectron Spectroscopy (XPS) measurements were performed and the intensities of the atomic concentrations were determined by numerical integration of the relative peaks. The formation of the SAMs using different alkanethiols was confirmed by tracking the changes of the C1s, N1s and O1 values. N1s element was not observed on carboxyl terminated SAM surface and also not in the antibody covered surface because of the head on positioning of the antibody. But since the streptavidin-biotin relationship switches the positioning of the antibody from tail-on to head-on positioning, N1s element was observed on the bioaffinity attachment method.

Table 3.2 X-RAY Photoelectron Spectroscopy (XPS) results for alkanethiols

Elemental Compositions	Au4f	C1s	O1	N1s
4-ATP	50.1	43.6	0.1	6.3
4-ATP+EpCAM	26.6	59.3	4.2	9.9
11-AUT	22.8	62.6	4	10.6
11-AUT+EpCAM	24.5	64.4	2.8	8.4
11-MUA	33.6	65.9	0.1	—
11-MUA+EpCAM	32.2	67.1	0.1	—
11-MUA+Strep+B.EpCAM	9.8	57.7	21.6	10.9

Change in the wettability after the SAM formation of alkanethiols and the immobilization of EpCAM antibody were examined with contact angle measurements with freshly prepared samples. The water contact angle on bare gold surface was measured as 45°. When SAM of 11-MUA was formed, this angle decreased down to 41°±2. After antibodies were immobilized on 11-MUA modified surfaces, the angle increased to 43°±2 but when biotinylated antibody used onto streptavidin modified 11-MUA surface, hydrophilicity increased to 41° because of the polar ureido-tetrahydrothiophene rings of biotin [89]. In the cases of amine terminated alkanethiols, the angle increased with the formation of SAMs because of the creation hydrophobic groups on the surface. Namely, for 11-AUT and 4-ATP the angles were measured as 53°±1 and 52°±2, respectively. When the EpCAM antibodies were immobilized, 11-AUT and 4-ATP and became 51°±4 and 53°±3, respectively. So, when carboxyl groups were created on the surface, the hydrophilic character was increased. This increase is in good agreement with the literature [84,90,91].

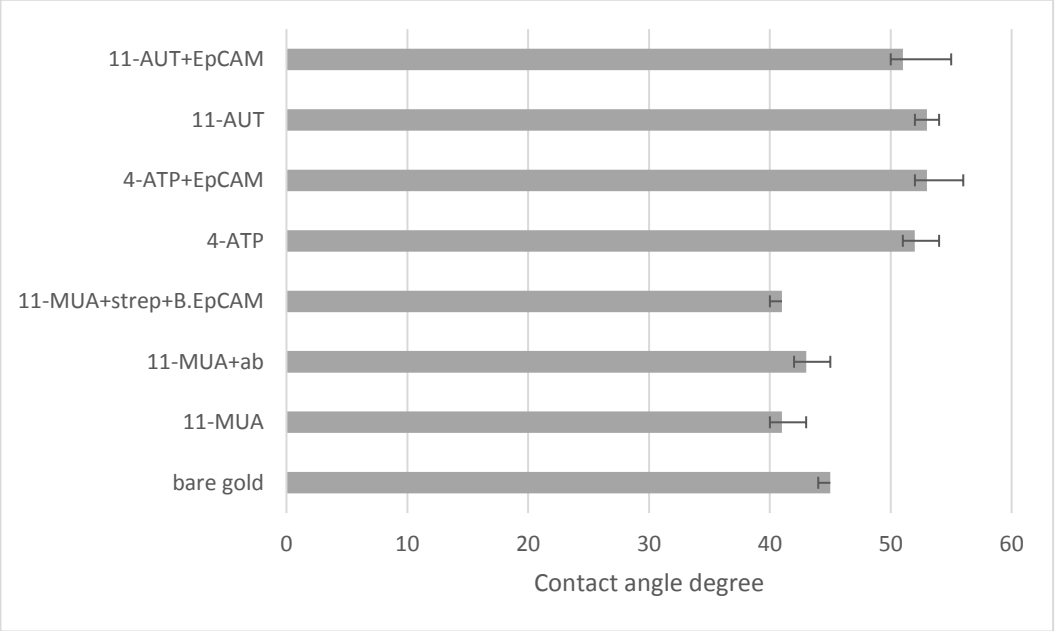

Figure 3-22 Contact angle measurement values of the alkanethiol modified surfaces

3.3.2. PEG-Thiol Studies

For the PEG thiol SAM formed and antibody attached surfaces, Atomic Force Microscopy (AFM) imaging was performed. The root mean square (RMS) roughness values were found to be 1.44±0.01nm, 1.09 nm and 1.64 nm for SAMs created with PEG-COOH, PEG-MIX and PEG-NH2 respectively. These values were changed to 1.27 nm, 2.05±0.02 nm and 1.08±0.06 nm after the antibody immobilization. For the bioaffinity method, PEG-COOH surfaces RMS values changed to 1.40±0.01 nm.

These values show how the PEG-CH3 inhibits the antibody immobilization and creates an uneven surface when combined with PEG-COOH (Figure 3.23).

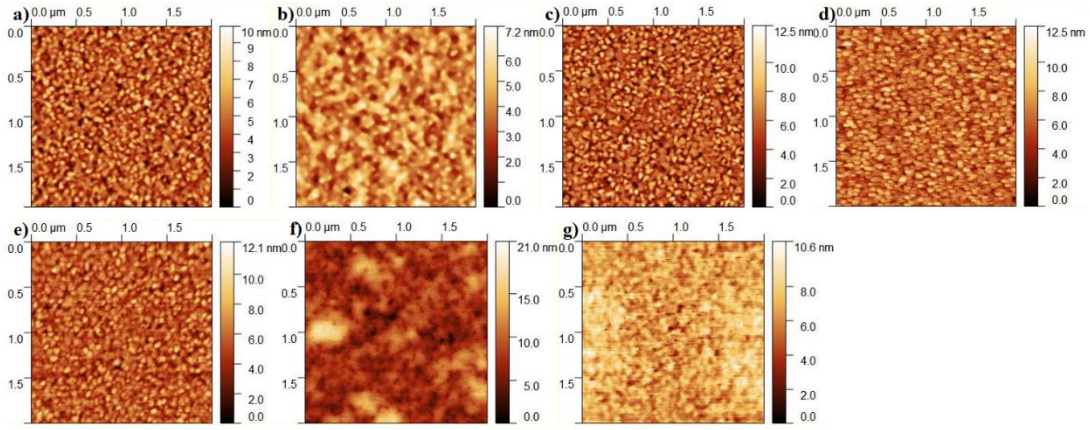

Figure 3.23 AFM images of SAM formed with a)PEG-COOH b) PEG-COOH:PEG-CH_3 Mixture c)PEG-NH_2, biotinylated antibodies immobilized on surfaces with d) PEG-COOH and antibodies covalently immobilized on surfaces with e) PEG-COOH f) PEG-COOH:PEG-CH_3 mixture g) PEG-NH_2

Elemental composition of each surface modification strategy analyzed with X-RAY Photoelectron Spectroscopy (XPS) and as expected N1s element was only observed on antibody covered SAM surfaces. The results also show irregular PEG structure by not showing N1s on the immobilized surface of PEG-NH_2. In addition, since the PEG-MIX allows only limited amount of antibody coverage, N1s element was not observed on the surface (Table 3.3).

Table 3.3 X-RAY Photoelectron Spectroscopty (XPS) results for PEG-thiols

Elemental Compositions	Au4f	C1s	O1	N1s	I3O5
PEG-NH_2	38.3	61.7	<.1	—	—
PEG-NH_2+EpCAM	18.5	72.9	<.1	7.8	0.8
PEG-MIX	22.7	77.3	<.1	—	—
PEG-MIX+EpCAM	13.4	85.9	<.1	—	0.7
PEG-COOH	39.1	60.9	<.1	—	—
PEG-COOH+EpCAM	21.7	65.3	<.1	11.5	1.5
PEG-COOH+Strep+B.EpCAM	12.7	72.9	0.3	14.9	—

The water contact angle results for the PEG-thiol surfaces was mesures for PEG-COOH as 40±7 and after EpCAM antibody immobilization the result did not changed, but after the biotinylated EpCAM antibody immobilization, it increased to 47±2. For the PEG-NH_2 the measurement was 53±4 and after the antibody immobilization it increased to 59±4. For the PEG-COOH: PEG-CH_3 it measured as 46±1 and increased highly to 60±4.

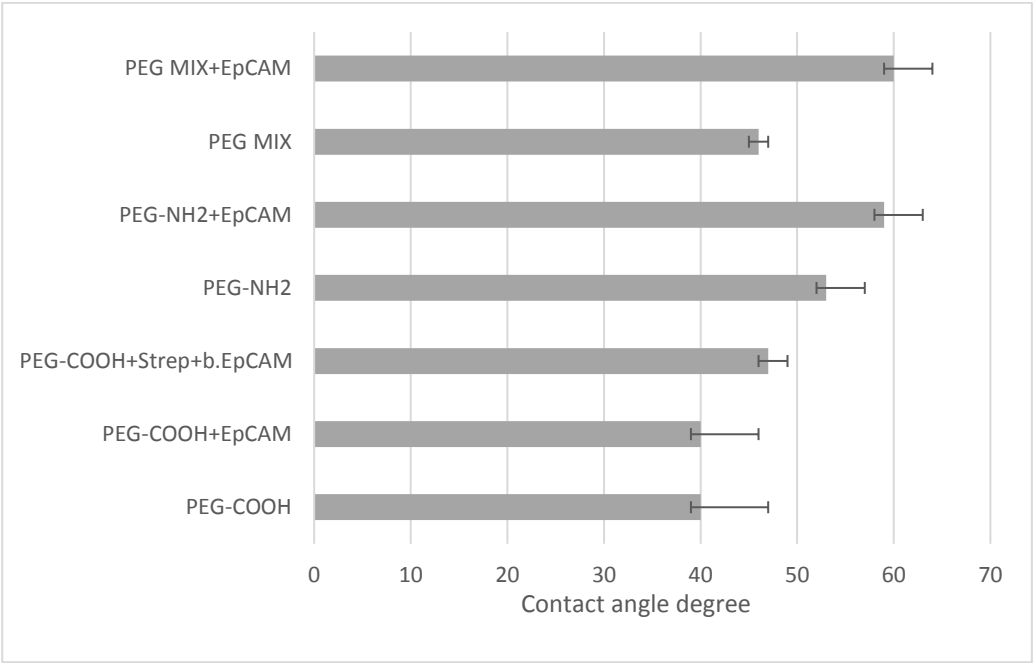

Figure 3.24 Contact angle measurement values of the PEG thiol modified surfaces

CHAPTER 4

DISCUSSION

In this thesis report, the affinities of the epithelial origin CTCs to anti-EpCAM antibody was used as the primary strategy. Although EpCAM is one of the most popularly studied antibody in the CTC isolation and identification researches, it is not the only option as in mentioned earlier in Chapter 1. But there are two reason why EpCAM antibody was chosen for this study; first it is rather cost-efficient when ensuring that the MCF-7 is an epithelial origin cell line and second, it has been employed both in various scientific and commercially available devices, such as CellSearch® Platform. Also, in this study, MCF-7 breast cancer cell line used as model CTC, by ignoring other epithelial origin CTCs that have different EpCAM expression levels, because breast cancer has the highest death and new cases rate in women all around the world. Further, the tests that conducted with the K562 leukemia cell line proved that there exists a specific interaction between the immobilized EpCAM antibodies and the epithelial origin CTC model MCF-7 cells. Overall, the main goal of the thesis was to search the surface modification molecules that used in this field which gives the maximum CTC attachment. Any kind of antibody and CTC type can be further studied with the desired surface modification molecules.

Another critical issue in the microfluidic studies is the flow rate. The high throughput is essential for the POC devices, but the cell experiences severe deformations when subjected to high shear stress. The focus, throughout the study, was to implement the surface modification strategies into microfluidic devices directly. For this, a very basic and plain channel design was used only to test whether those strategies worked well or not and to what expend they gave successful results. There is a need in the market for the cell attachment in dynamic flow and related future works should be performed to employ other relevant CTC capture analysis for further studies.

While testing the bare gold surfaces, it was found that the short chained alkanethiols were giving less cell attachment compared to longer chained alkanethiols. The reason for the insufficient capture for the short carbon chain molecules is believed to be due to the steric hindrance effect. Since 3-MPA molecule is very short with its three atoms, it is possible to limit the immobilized antibody amount and the captured CTC amount. Molecules could stay too close to one other and form a dense and heterogeneous surface [72,79,80]. Also, this heterogeneous surface could bring high nonspecific attachments on 3-MPA surfaces [60]. On the other hand, 11-MUA shows high CTC capture because long chained alkanethiols create strong Van der Waals forces between their chains and causes to form dense and well-ordered brush like structures [81, 82].

Same as the 3-MPA, amine terminated two carbon Cys molecule is too short to form a homogeneous layer. On the other hand, the CTC capture in the other two cases, especially in 4-ATP, were quite high. Since 4-ATP molecule contains a phenol ring, the activated sites of the molecule stay far away from each other compared to the distance occur when using Cys. Also, it has been shown that aromatic ring containing thiols permits high ordering via π-π interactions, which also increase the stability and rigidity of SAM compared to alkyl based SAMs [83]. This prevents the heterogeneity and leading to maximum CTC capture. 11-AUT also yielded a high amount of CTC capture like 11-MUA but when it is compared with 11-MUA, 11-AUT resulted in better capture. This is believed to be resulting from the EpCAM antibody positioning. In order to effectively benefit from an antibody, it should be structurally allowing the target to sit on. This is accomplished by correctly positioning the antibody [81,84].

For improving the affinity and the stability of the cell attachment, the final orientation of the antibodies was studied. The molecular interaction between the paratope on the antibody and epitope on the antigen was observed via immobilizing the antibodies on SAMs either in ‘head on’ and ‘tail on’ positions. Antibody orientation changed by the

covalent and bioaffinity binding and the cell attachment performances on the same molecule was observed according to the yielding orientation.

When bioaffinity method compared to the covalent method, it provides more cell attachment on low concentration SAM surfaces. The possible reason could be the nonhomogeneous immobilization of the streptavidin molecules on the crowded SAM layer [86]. Therefore, when using streptavidin-biotin interaction technique, lower SAM concentrations were employed [64, 87].

The significant number of biotechnological applications demands surfaces with defined regions of various chemical functionalities to minimize undesired surface interactions while ensuring binding of desired species to specific regions. Since gold regions have affinity for proteins, false positive signals could be reduced using PEG thiols which reduces the nonspecific cell and protein adhesion. One of the most popular water soluble polymer PEG could be used by changing its terminal group to attach required antibodies while its backbone provides protein repelling behavior. PEG-CH_3 could be used as a blocking agent, as an alternative to BSA and ethanolamine. In order to construct more specific biorecognition site and in case of needing less dense cell adhesion on the surface, PEG-CH_3 can be mixed with other PEG thiols. Also, one of the downsides of the alkanethiols was eliminated with the high performance of PEG thiols under 3-hour incubation.

CHAPTER 5

CONCLUSION

In this study, CTC model MCF-7 cell capture comparison was carried out by immobilizing EpCAM antibodies on different SAM modified gold surfaces. Mainly, covalent and bioaffinity bindings were employed to immobilize antibodies. characterization was made with AFM, XPS and contact angle measurements. For the covalent bindings cysteamine, 11-mercaptoundecanoic acid, 3-mercaptopropionic acid, 4-aminothiophenol, 11-mercapto-1-undecanethiol, HS-PEG-NH_2 and HS-PEG-COOH used as thiol molecules in order to create SAMs. Within these 11-mercaptoundecanoic acid and HS-PEG-COOH used for the bioaffinity based antibody immobilization. On the antibody bonded surfaces, cell attachment events were monitored using fluorescence microscopy imaging. In order to investigate the selectivity of the functionalized surfaces, EpCAM positive MCF-7 and EpCAM negative K562 cell lines were used. Testing the methods on the glass and parylene allowed the investigation of the specificity of the procedures towards gold. Studies showed long alkanethiols and aromatic ring lead to better cell capture events than shorter alkanethiols on gold surfaces. For the improvement of eliminating the nonspecific bindings PEG thiols could also be used for creating a thiol end on the gold surfaces. It was confirmed, that the antibody positioning holds a significant impact since the cell capture can be performed best at tail-on position, which can be provided only with the amine terminated SAMs. All the methods were also successfully implemented in microchannel, but the microchannel designs that used in this study was only allowing laminar flow, hence the cell attachments were only performed through incubation. Results obtained from the comparisons holds a great importance for the gold surface-based biosensor designs that are aimed for CTC detection.

REFERENCES

[1] Kohler BA, Ward EM, et al. “Global Cancer Facts & Figures.” American Cancer Society. J Natl Cancer Inst. 2011; 103:123.

[2] “Cancer Diagnostics Market Size, Industry Analysis Report.”, 2019-2026, Report ID: GVR-1-68038-213-6.

[3] J. Flaherty, S. Gray, D. Richard et al., 2012. Lung Cancer Circulating tumour cells, their role in metastasis and their clinical utility in lung cancer, Lung Cancer, 76, 19-25p. doi:10.1016/j.lungcan.2011.10.018.

[4] C.L. Chaffer, R.A. Weinberg, 2011. A Perspective on Cancer Cell Metastasis, Science (80-). 331 (2011) 1559 LP-1564. doi:10.1126/science.1203543.

[5] D. Wirtz, K. Konstantopoulos, and P. C. Searson, “The physics of cancer: the role of physical interactions and mechanical forces in metastasis,” Nat Rev Cancer, vol. 11, no. 7, pp. 512–522, Jun. 2011.

[6] C. Criscitiello, F. André, A.M. Thompson, M. De Laurentiis, A. Esposito, L. Gelao, L. Fumagalli, M. Locatelli, I. Minchella, F. Orsi, A. Goldhirsch, G. Curigliano, Biopsy confirmation of metastatic sites in breast cancer patients: Clinical impact and future perspectives, Breast Cancer Res. 16 (2014). doi:10.1186/bcr3630.

[7] T. Foukakis, G. Åström, L. Lindström, T. Hatschek, J. Bergh, When to order a biopsy to characterise a metastatic relapse in breast cancer, Ann. Oncol. 23 (2012). doi:10.1093/annonc/mds297.

[8] M. Ilié, P. Hofman, Pros: Can tissue biopsy be replaced by liquid biopsy?, Transl. Lung Cancer Res. 5 (2016) 420–423. doi:10.21037/tlcr.2016.08.06.

[9] May, Charles D., et al. "Procedures for immunochemical study of histamine release from leukocytes with small volume of blood." Journal of Allergy 46.1 (1970): 12-20.doi: 10.1016/0021-8707(70)90056-0.

[10] J.D.O. Flaherty, S. Gray, D. Richard, D. Fennell, J.J.O. Leary, F.H. Blackhall, K.J.O. Byrne, Circulating tumour cells , their role in metastasis and their clinical utility in lung cancer, Lung Cancer. 76 (2012) 19–25. doi:10.1016/j.lungcan.2011.10.018.

[11] M. Fleischhacker, B. Schmidt, Circulating nucleic acids (CNAs) and cancer, A survey, 1775 (2007) 181–232. doi:10.1016/j.bbcan.2006.10.001.

[12] S. Calabuig-fariñas, E. Jantus-lewintre, A. Herreros-pomares, C. Camps, Circulating tumor cells versus circulating tumor DNA in lung cancer, which one will win ?, 5 (2016) 466–482. doi:10.21037/tlcr.2016.10.02.

[13] C. Rajagopal, K.B. Harikumar, The Origin and Functions of Exosomes in Cancer, 8 (2018). doi:10.3389/fonc.2018.00066.

[14] H. Bu, D. He, X. He, K. Wang, Exosomes : Isolation , Analysis , and Applications in Cancer Detection and Therapy, (2018) 1–12. doi:10.1002/cbic.201800470.

[15] H. Esmaeilsabzali, T. V. Beischlag, M.E. Cox, A.M. Parameswaran, E.J. Park, Detection and isolation of circulating tumor cells: Principles and methods, Biotechnol. Adv. 31 (2013) 1063–1084. doi:10.1016/j.biotechadv.2013.08.016.

[16] B. Mostert, S. Sleijfer, J.A. Foekens, J.W. Gratama, Circulating tumor cells (CTCs): Detection methods and their clinical relevance in breast cancer, Cancer Treat. Rev. 35 (2009) 463–474. doi:10.1016/j.ctrv.2009.03.004.

[17] M. Kalinich, I. Bhan, T.T. Kwan, D.T. Miyamoto, S. Javaid, J.A. Licausi, An RNA-based signature enables high specificity detection of circulating tumor cells in hepatocellular carcinoma, (2016). doi:10.1073/pnas.1617032114.

[18] S.S. Shevkoplyas, T. Yoshida, L.L. Munn, M.W. Bitensky, Biomimetic Autoseparation of Leukocytes from Whole Blood in a Microfluidic Device, 77 (2005) 933–937.

[19] S.M. McFaul, B.K. Lin, H. Ma, Cell separation based on size and deformability using microfluidic funnel ratchets, Lab Chip. 12 (2012) 2369–2376. doi:10.1039/c2lc21045b.

[20] W. Qian, Y. Zhang, W. Chen, Capturing Cancer: Emerging Microfluidic Technologies for the Capture and Characterization of Circulating Tumor Cells, Small. 11 (2015) 3850–3872. doi:10.1002/smll.201403658.

[21] V. Murlidhar, L. Rivera-Báez, S. Nagrath, Affinity Versus Label-Free Isolation of Circulating Tumor Cells: Who Wins?, Small. 12 (2016) 4450–4463. doi:10.1002/smll.201601394.

[22] J.S. Kuo, Y. Zhao, P.G. Schiro, L. Ng, D.S.W. Lim, J.P. Shelby, D.T. Chiu, Deformability considerations in filtration of biological cells †, 10 (2010). doi:10.1039/b922301k.

[23] H.A. Pohl, Continuous Dielectrophoretic Separation of Cell Mixtures, 28 (1979) 15–28 doi:10.1007/BF02785053.

[24] M. Alshareef et al., "Separation of tumor cells with dielectrophoresis-based microfluidic chip," Biomicrofluidics, vol. 7, no. 1, 2013.

[25] F. F. Becker, X. Wang, Y. Huang, R. Pethigt, J. Vykoukal, and P. R. C. Gascoyne, "Separation of human breast cancer cells from blood by differential dielectric affinity," vol. 92, no. January, pp. 860–864, 1995.

[26] P.R.C. Gascoyne, S. Shim, Isolation of Circulating Tumor Cells by Dielectrophoresis, (2014) 545–579. doi:10.3390/cancers6010545.

[27] Z. Wu, Microfluidic Hydrodynamic Cell Separation : A Review Microfluidic Hydrodynamic Cell Separation : A Review, Micro and Nanosystems, (2009), vol.1, pp181.

[28]Y. Gou, Y. Jia, P. Wang, C. Sun, Progress of Inertial Microfluidics in Principle, (2018). doi:10.3390/s18061762.

[29] J. Zhang, D. Yuan, Fundamentals and applications of inertial microfluidics : A review, 16 (2016) 10–34.

[30] R.G. Tompkins, M.R. Smith, S. Nagrath, A. Muzikansky, S. Digumarthy, P. Ryan, L. V. Sequist, L. Ulkus, D. Irimia, S. Maheswaran, M. Toner, D.W. Bell, U.J. Balis, D.A. Haber, E.L. Kwak, Isolation of rare circulating tumour cells in cancer patients by microchip technology, Nature. 450 (2007) 1235–1239. doi:10.1038/nature06385.

[31] D.I. Tsukrov, B.A. Waltman, G.K. Korir, M. Toner, R.J. Lee, D. Winokur, D.T. Miyamoto, S.M. Rothenberg, A.M. Shah, D.A. Haber, S.L. Stott, M.E. Smas, K.J. Isselbacher, S. Springer, M. Yu, F.P. Floyd, L. V. Sequist, D. Irimia, C.-H. Hsu, S. Nagrath, S. Maheswaran, A.J. Gilman, J.B. Lord, Isolation of circulating tumor cells using a microvortex-generating herringbone-chip, Proc. Natl. Acad. Sci. 107 (2010) 18392–18397. doi:10.1073/pnas.1012539107.

[32] W.T. Ye Xu, Joseph A. Phillips, Jilin Yan, Qingge Li, Z. Hugh Fan, Y. Xu, J.A. Phillips, J. Yan, Q. Li, Z.H. Fan, W. Tan, P.O. Box, Aptamer-based microfluidic device for enrichment, sorting, and detection of multiple cancer cells, Anal. Chem. 81 (2011) 7436–7442. doi:10.1021/ac9012072.Aptamer-based.

[33] X. Mao, Y. Ma, A. Zhang, L. Zhang, L. Zeng, and G. Liu, Anal. Chem. 81, 1660–1668 (2009).

[34] A. V. Lakhin, V.Z. Tarantul, L. V. Gening, Aptamers : Problems, solutions and prospects, Acta Naturae. 5 (2013) 34–43.

[35] J. Hidding, A therapeutic battle : Antibodies vs . Aptamers, (n.d.) 1–20.

[36] Linda C Griffin, George F Tidmarsh, Louis C Bock, John J Toole, and LL Leung. In vivo anticoagulant properties of a novel nucleotide-based thrombin inhibitor and demonstration of regional anticoagulation in extracorporeal circuits. Blood, 81(12):3271–3276, 1993.

[37] L. C. Griffin, G. F. Tidmarsh, L. C. Bock, J. J. Toole, L. L. Leung, Blood 1993, 81, 3271 ± 3276.

[38] D. Eulberg, S. Klussmann, Spiegelmers: Biostable aptamers, ChemBioChem. 4 (2003) 979–983. doi:10.1002/cbic.200300663.

[39] H.H. Cai, Therapeutic monoclonal antibodies approved by FDA in 2017, 1 (2018) 2017–2019. doi:10.15406/moji.2018.06.00198.

[40] Schmidt, M. et al. (2008) Prognostic effect of epithelial cell adhesion molecule overexpression in untreated node-negative breast cancer. Clin. Cancer Res., 14, 5849–5855.

[41] Piyathilake, C.J. et al. (2000) The expression of Ep-CAM (17-1A) in squamous cell cancers of the lung. Hum. Pathol., 31, 482–487.

[42] Herlyn, M. et al. (1979) Colorectal carcinoma-specific antigen: detection by means of monoclonal antibodies. Proc. Natl Acad. Sci. USA., 76, 1438– 1442.

[43] B.T.F. van der Gun, L.J. Melchers, M.H.J. Ruiters, L.F.M.H. de Leij, P.M.J. McLaughlin, M.G. Rots, EpCAM in carcinogenesis: The good, the bad or the ugly, Carcinogenesis. 31 (2010) 1913–1921. doi:10.1093/carcin/bgq187.

[44] M. Trzpis, P.M.J. McLaughlin, L.M.F.H. De Leij, M.C. Harmsen, Epithelial cell adhesion molecule: More than a carcinoma marker and adhesion molecule, Am. J. Pathol. 171 (2007) 386–395. doi:10.2353/ajpath.2007.070152.

[45] A. Arbor, M. Zeinali, D.A. Arbor, D.M. Simeone, HHS Public Access, 10 (2015) 4895–4904. doi:10.1002/smll.201400719.A.

[46] S. M. Santana, H. Liu, N. H. Bander, J. P. Gleghorn, B. J. Kirby, Biomed. Microdevices 2012, 14, 401.

[47] J.P. Gleghorn, E.D. Pratt, D. Denning, H. Liu, N.H. Bander, S.T. Tagawa, D.M. Nanus, A. Giannakakou, B.J. Kirby, Capture of circulating tumor cells from whole blood of prostate cancer patients using geometrically enhanced differential

immunocapture (GEDI) and a prostate-specific antibody †, (2010) 27–29. doi:10.1039/b917959c.

[48] R.L. Bitting, R. Boominathan, C. Rao, G. Kemeny, B. Foulk, M.A. Garcia-Blanco, M. Connelly, A.J. Armstrong, Development of a method to isolate circulating tumor cells using mesenchymal-based capture, Methods. 64 (2013) 129–136. doi:10.1016/j.ymeth.2013.06.034.

[49] C. Birtolo, H. Pham, S. Morvaridi, C. Chheda, V.L.W. Go, A. Ptasznik, M. Edderkaoui, M.H. Weisman, E. Noss, M.B. Brenner, B. Larson, M. Guindi, Q. Wang, S.J. Pandol, Cadherin-11 Is a Cell Surface Marker Up-Regulated in Activated Pancreatic Stellate Cells and Is Involved in Pancreatic Cancer Cell Migration, Am. J. Pathol. 187 (2017) 146–155. doi:10.1016/j.ajpath.2016.09.012

[50] D.R. Beier, NIH Public Access, 61 (2015) 230–233. doi:10.1002/0471142905.hg1504s82.ENU

[51] Tamura D, Hiraga T, Myoui A, Yoshikawa H, Yoneda T: Cadherin11-mediated interactions with bone marrow stromal/osteoblastic cells support selective colonization of breast cancer cells in bone. Int J Oncol 2008, 33:17e24.

[52] Satcher RL, Pan T, Cheng CJ, Lee YC, Lin SC, Yu G, Li X, Hoang AG, Tamboli P, Jonasch E, Gallick GE, Lin SH: Cadherin-11 in renal cell carcinoma bone metastasis. PLoS One 2014, 9: e89880.

[53] Lin YL, Gui SL, Ma JG: Aberrant methylation of CDH11 predicts a poor outcome for patients with bladder cancer. Oncol Lett 2015, 10: 647e652.

[54] Sagvolden, G.; Giaever, I.; Pettersen, E.O.; Feder, J. Cell adhesion force microscopy. Proc. Natl. Acad. Sci. USA 1999, 96, 471–476.

[55] Saif, M.A.T.; Sager, C.R.; Coyer, S. Functionalized biomicroelectromechanical systems sensors for force response study at local adhesion sites of single living cells on substrates. Ann. Biomed. Eng. 2003, 31, 950–961.

[56] Huang, W.; Anvari, B.; Torres, J.H.; LeBaron, R.G.; Athanasiou, K.A. Temporal effects of cell adhesion on mechanical characteristics of the single chondrocyte. J. Orthop. Res. 2003, 21, 88–95.

[57] S. Hong, E. Ergezen, R. Lec, K.A. Barbee, Real-time analysis of cell-surface adhesive interactions using thickness shear mode resonator, Biomaterials. 27 (2006) 5813–5820. doi:10.1016/j.biomaterials.2006.07.031.

[58] A.A. Khalili, M.R. Ahmad, A Review of cell adhesion studies for biomedical and biological applications, Int. J. Mol. Sci. 16 (2015) 18149–18184. doi:10.3390/ijms160818149.

[59] Y. Xue, X. Li, H. Li, W. Zhang, Quantifying thiol-gold interactions towards the efficient strength control, Nat. Commun. 5 (2014) 1–9. doi:10.1038/ncomms5348

[60] E. Baldrich, O. Laczka, F.J. Del Campo, F.X. Muñoz, Self-assembled monolayers as a base for immunofunctionalisation: Unequal performance for protein and bacteria detection, Anal. Bioanal. Chem. 390 (2008) 1557–1562. doi:10.1007/s00216-008-1887-1.

[61] A.K. Trilling, J. Beekwilder, H. Zuilhof, Antibody orientation on biosensor surfaces: A minireview, Analyst. 138 (2013) 1619–1627. doi:10.1039/c2an36787d.

[62] Y. Xue, X. Li, H. Li, W. Zhang, Quantifying thiol-gold interactions towards the efficient strength control, Nat. Commun. 5 (2014) 1–9. doi:10.1038/ncomms5348.

[63] Michel Godin, P.J. Williams, Vincent Tabard-Cossa, Olivier Laroche, L. Y. Beaulieu, R. B. Lennox, and Peter Grütter Langmuir 20, 7090 (2004), Langmuir, 2004, 20177090-7096, doi: 10.1021/la030257l.

[64] M. Seifert, M.T. Rinke, H. Galla, Characterization of Streptavidin Binding to Biotinylated, Binary Self- Assembled Thiol Monolayers; Influence of Component Ratio and Solvent, 26 (2010) 6386–6393. doi:10.1021/la904087s.

[65] David Pressman and Allan L Grossberg. Structural basis of antibody specificity. Benjamin, 1968 ayni P. Press, G. Britain, M. Biology, Book reviews, 5 (1968) 607–608.

[66] Roberto Reverberi and Lorenzo Reverberi. Factors affecting the antigen-antibody reaction. Blood Transfusion, 5(4):227, 2007.

[67] E. Ostuni, L. Yan, G.M. Whitesides, The interaction of proteins and cells with self-assembled monolayers of alkanethiolates on gold and silver, 15 (1999) 3–30.

[68] P. Kingshott, H.J. Griesser, Surfaces that resist bioadhesion, 4 (1999) 403–412.

[69] S. Choi, J. Chae, Methods of reducing non-specific adsorption in microfluidic biosensors, J. Micromechanics Microengineering. 20 (2010). doi:10.1088/0960-1317/20/7/075015

[70] I.S. Theory, Protein-Surface Interactions in the Presence of Polyethylene Oxide, 142 (1991).

[71] S. Asiaei, P. Nieva, M.M. Vijayan, Fast Kinetics of Thiolic Self-Assembled Monolayer Adsorption on Gold : Modeling and Con fi rmation by Protein Binding, (2014). doi:10.1021/jp509986s.

[72] P. Bhadra, M.S. Shajahan, E. Bhattacharya, A. Chadha, Studies on varying n-alkanethiol chain lengths on a gold coated surface and their effect on antibody-antigen binding efficiency, RSC Adv. 5 (2015) 80480–80487. doi:10.1039/c5ra11725a

[73] S.K. Arya, K.C. Lee, D. Bin Dah'Alan, Daniel, A.R.A. Rahman, Breast tumor cell detection at single cell resolution using an electrochemical impedance technique, Lab Chip. 12 (2012) 2362–2368. doi:10.1039/c2lc21174b.

[74] J. Wook, S. Jun, S. Min, J. Lee, Characterization of a self-assembled monolayer of thiol on a gold surface and the fabrication of a biosensor chip based on surface plasmon resonance for detecting anti-GAD antibody, 20 (2005) 1422–1427. doi:10.1016/j.bios.2004.04.017.

[75] S.H. Choi, J.W. Lee, S.J. Sim, Enhanced performance of a surface plasmon resonance immunosensor for detecting Ab – GAD antibody based on the modified self-assembled monolayers, 21 (2005) 378–383. doi: 10.1016/j.bios.2004.07.037.

[76] B.E. Kraziński, J. Radecki, H. Radecka, Surface plasmon resonance-based biosensors for exploring the influence of alkaloids on aggregation of amyloid-β peptide, Sensors. 11 (2011) 4030–4042. doi:10.3390/s110404030.

[77] A. Yadegari, M. Omidi, F. Yazdian, H. Zali, L. Tayebi, RSC Advances detection of cancer cells using modi fi ed graphene –, (2017) 2365–2372. doi:10.1039/C6RA25938C.

[78] M. Veiseh, B.T. Wickes, D.G. Castner, M. Zhang, Guided cell patterning on gold – silicon dioxide substrates by surface molecular engineering, 25 (2004) 3315–3324. doi:10.1016/j.biomaterials.2003.10.014.

[79] M. Wirde, U. Gelius, L. Nyholm, Self-assembled monolayers of cystamine and cysteamine on gold studied by XPS and voltammetry, Langmuir. 15 (1999) 6370–6378. doi:10.1021/la9903245.

[80] S. Subramanian, S. Sampath, Effect of chain length on the adhesion behaviour of n-alkanethiol self-assembled monolayers on Au (1 1 1): An atomic force microscopy study, 65 (2005) 753–761.

[81] S. Gaffar, R. Nurmalasari, Yohan, Y.W. Hartati, Voltammetric DNA Biosensor using Gold Electrode Modified by Self Assembled Monolayer of Thiol for Detection of Mycobacterium Tuberculosis, Procedia Technol. 27 (2017) 74–80. doi:10.1016/j.protcy.2017.04.034.

[82] J.C. Love, L.A. Estroff, J.K. Kriebel, R.G. Nuzzo, G.M. Whitesides, Self-Assembled Monolayers of Thiolates on Metals as a Form of Nanotechnology, 2005.

[83] E. Bedford, Effect of SAM chain length and binding functions on protein adsorption : β - Lactoglobulin and apo-transferrin on gold, (2015). doi:10.1016/j.colsurfb.2014.01.031.

[84] J. Cancino, S.A.S. MacHado, Microelectrode array in mixed alkanethiol self-assembled monolayers: Electrochemical studies, Electrochim. Acta. 72 (2012) 108–113. doi:10.1016/j.electacta.2012.04.009.

[85] N.G. Welch, J.A. Scoble, B.W. Muir, P.J. Pigram, Orientation and characterization of immobilized antibodies for improved immunoassays (Review), Biointerphases. 12 (2017) 02D301. doi:10.1116/1.4978435.

[86] A. Taninaka, O. Takeuchi, H. Shigekawa, Hidden variety of biotin – streptavidin / avidin local interactions revealed by site-selective dynamic force spectroscopy, (2010) 12578–12583. doi:10.1039/c0cp00259c.

[87] E. Araya, M.J. Kogan, A.G. Guell, C.A. Escobar, F. Sanz, Sensing immobilized molecules of streptavidin on a silicon surface by MALDI-TOF mass spectrometry and fluorescence microscopy, J. Chil. Chem. Soc. 59 (2014) 2458–2463. doi:10.4067/S0717-97072014000200013.

[88] H.W. M. Sprik, E. Delamarche, B. Michel, U. Roethlisberger, M. L. Klein, Structure of Hydrophilic Self-Assembled Monolayers: A Combined Scanning Tunneling Microscopy and Computer Simulation Study, Langmuir 1994 10 (11), 4116-4130. (n.d.).

[89] E.H. Williams, A. V Davydov, A. Motayed, S.G. Sundaresan, P. Bocchini, L.J. Richter, G. Stan, K. Steffens, R. Zangmeister, J.A. Schreifels, M. V Rao, Applied Surface Science Immobilization of streptavidin on 4H – SiC for biosensor development, Appl. Surf. Sci. 258 (2012) 6056–6063. doi:10.1016/j.apsusc.2012.02.137.

[90] N. Afara, S. Omanovic, M. Asghari-khiavi, Functionalization of a gold surface with fi bronectin (FN) covalently bound to mixed alkanethiol self-assembled monolayers (SAMs): The in fl uence of SAM composition on its physicochemical properties and FN surface secondary structure, Thin Solid Films. 522 (2012) 381–389. doi:10.1016/j.tsf.2012.08.025.

[91] M. Veiseh, M.H. Zareie, M. Zhang, Highly Selective Protein Patterning on Gold - Silicon Substrates for Biosensor Applications, 14 (2002) 6671–6678. doi:10.1021/la025529j.

APPENDICES

A. XPS Analysis Results

Change in the atomic composition of gold surfaces after each modification was measured by XPS analysis. The atomic orbital peaks of Au4f, C1s, O1 and N1s are given in the Figure S1-S7 for alkanethiol and antibody covered surfaces.

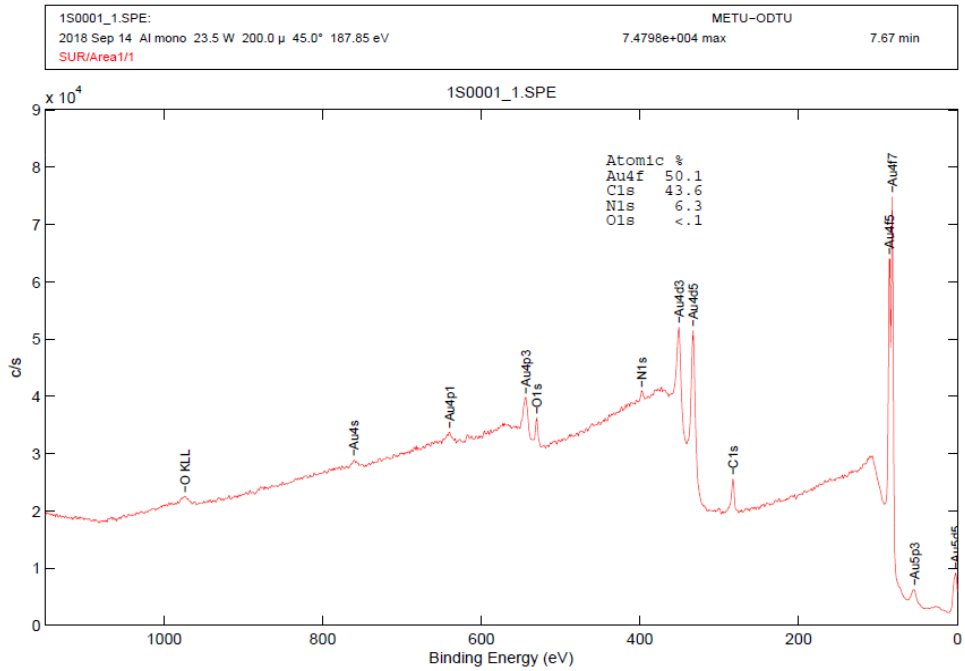

Figure S.1 XPS analysis for 4-ATP

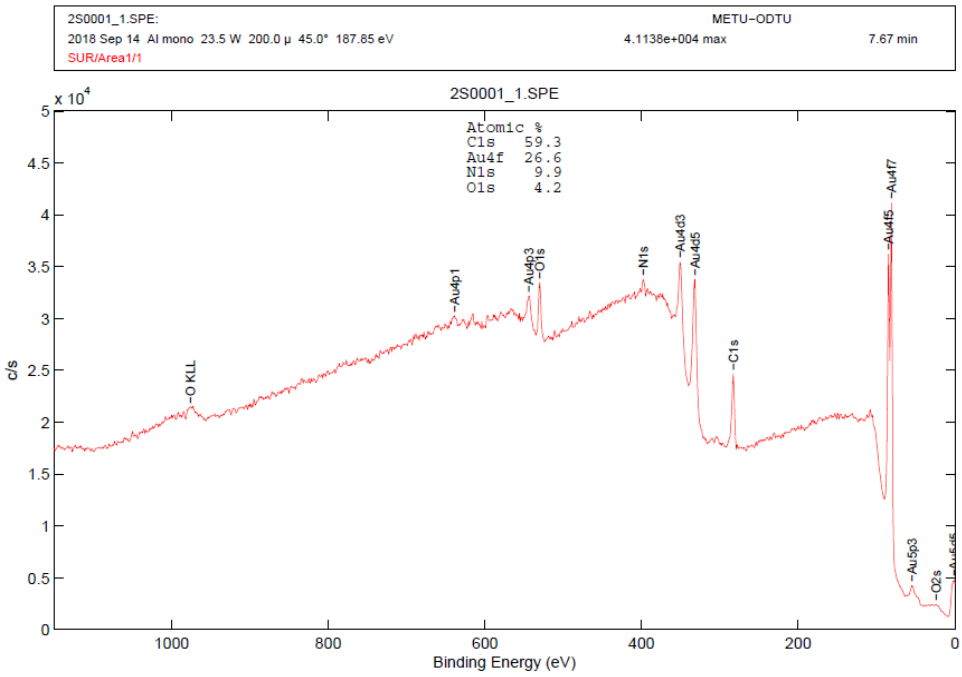

Figure S.2 XPS analysis for antibody covered 4-ATP surface

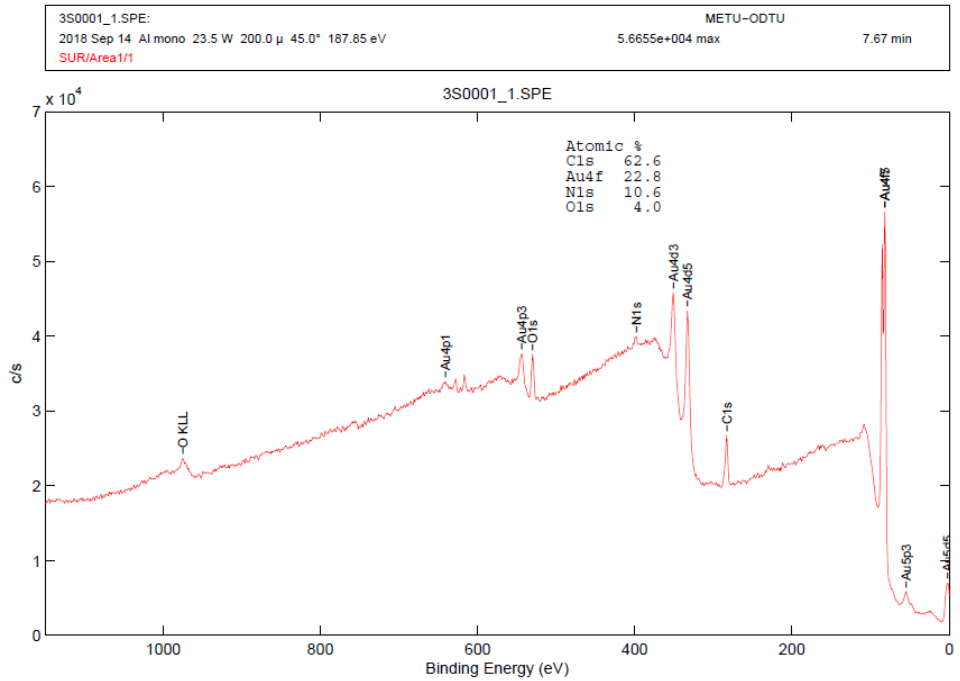

Figure S.3 XPS analysis for 11-AUT surface

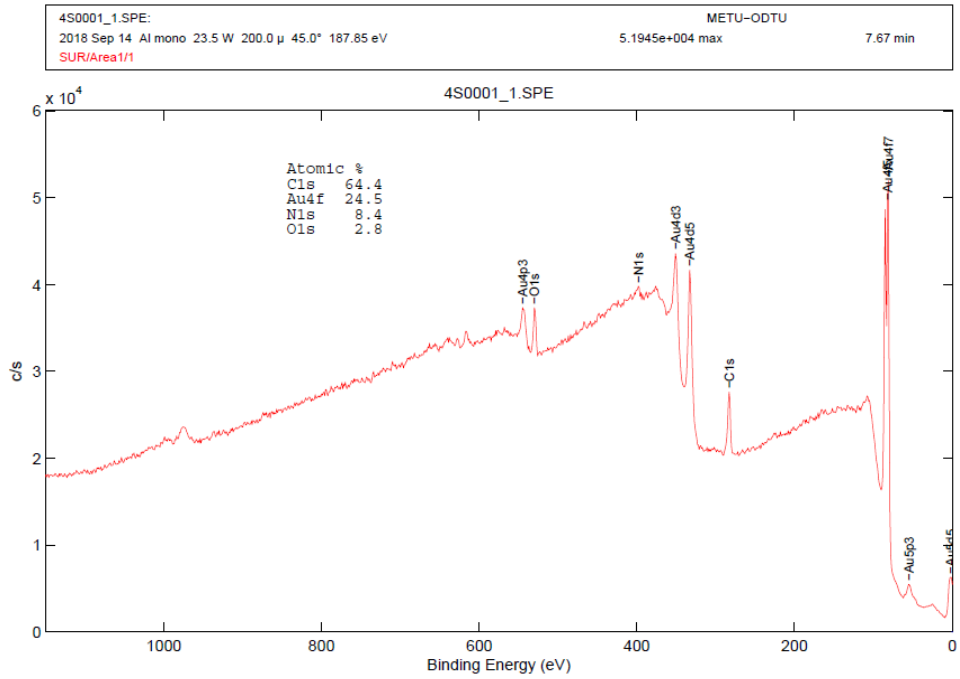

Figure S.4 XPS analysis for antibody covered 11-AUT surface

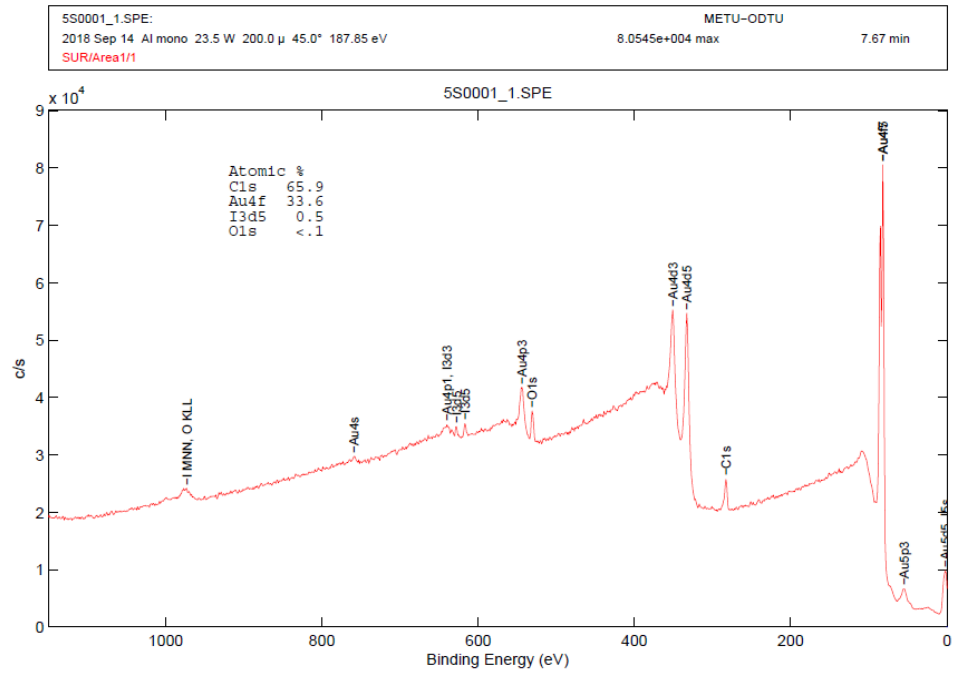

Figure S.5 XPS analysis for 11-MUA surface

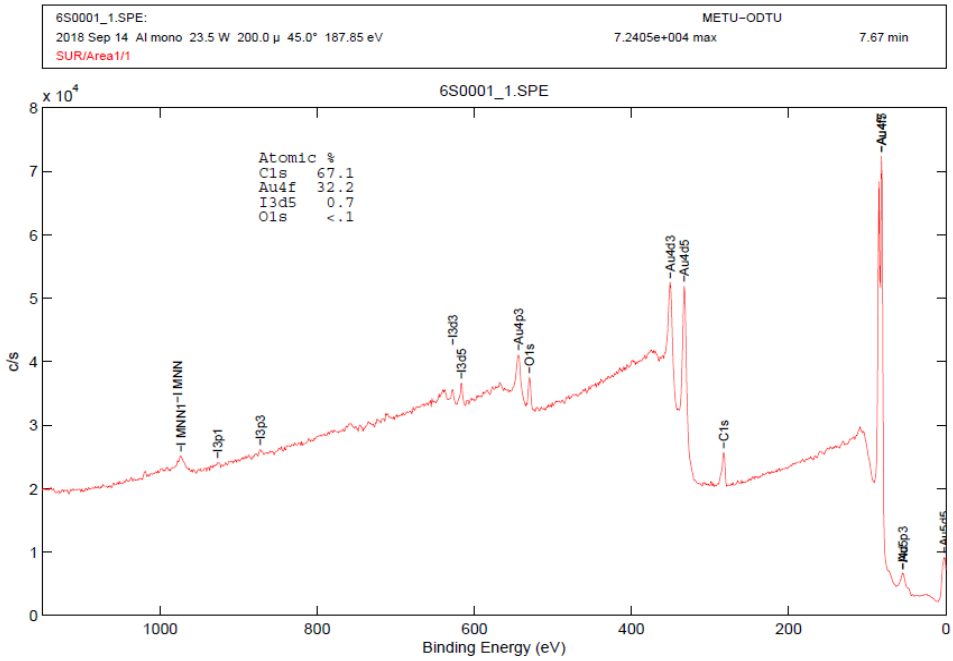

Figure S.6 XPS analysis for antibody covered 11-MUA surface

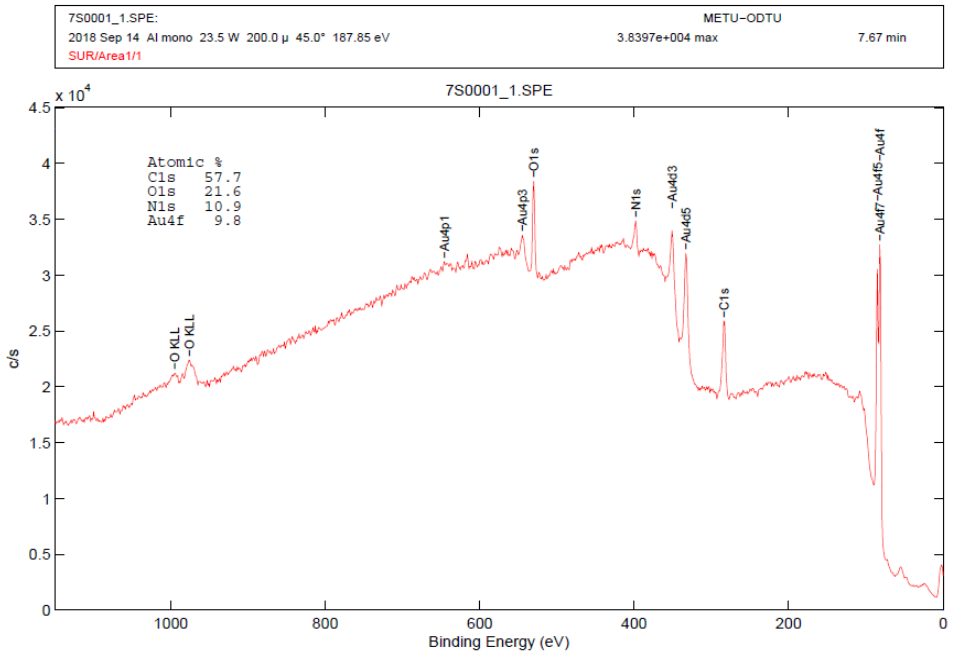

Figure S.7 XPS analysis for biotinylated antibody covered 11-MUA surface

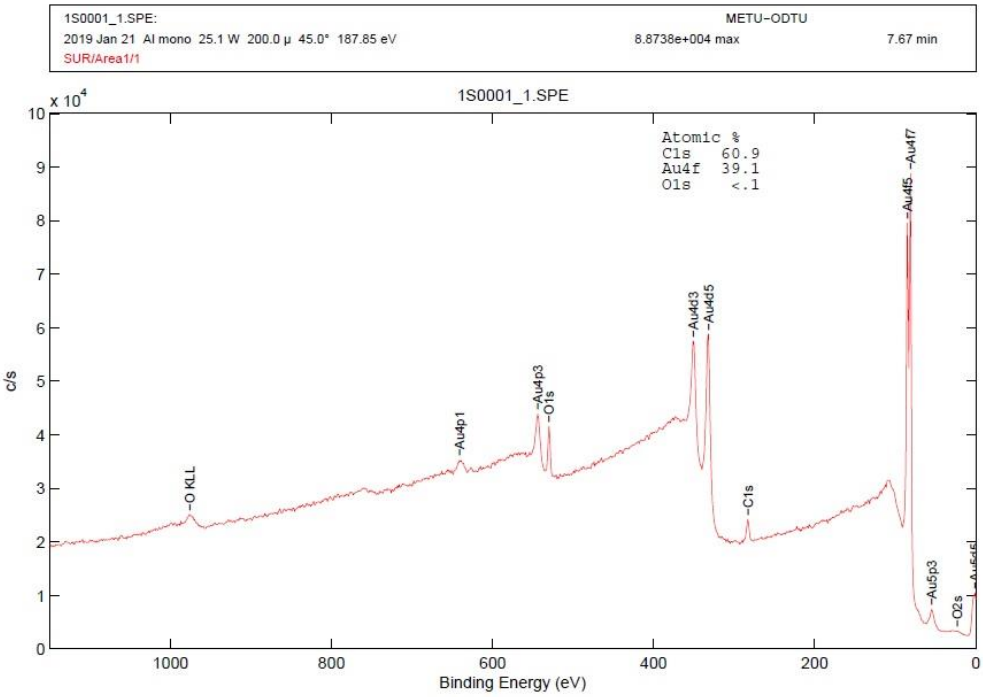

Figure S.8 XPS analysis for HS-PEG-COOH surface

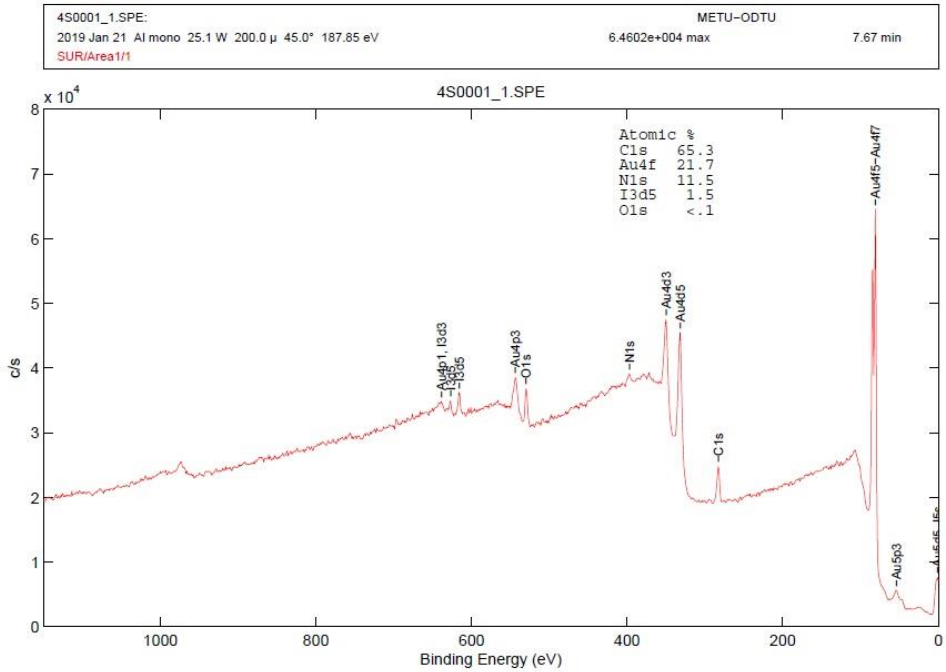

Figure S.9 XPS analysis of antibody covered HS-PEG-COOH surface

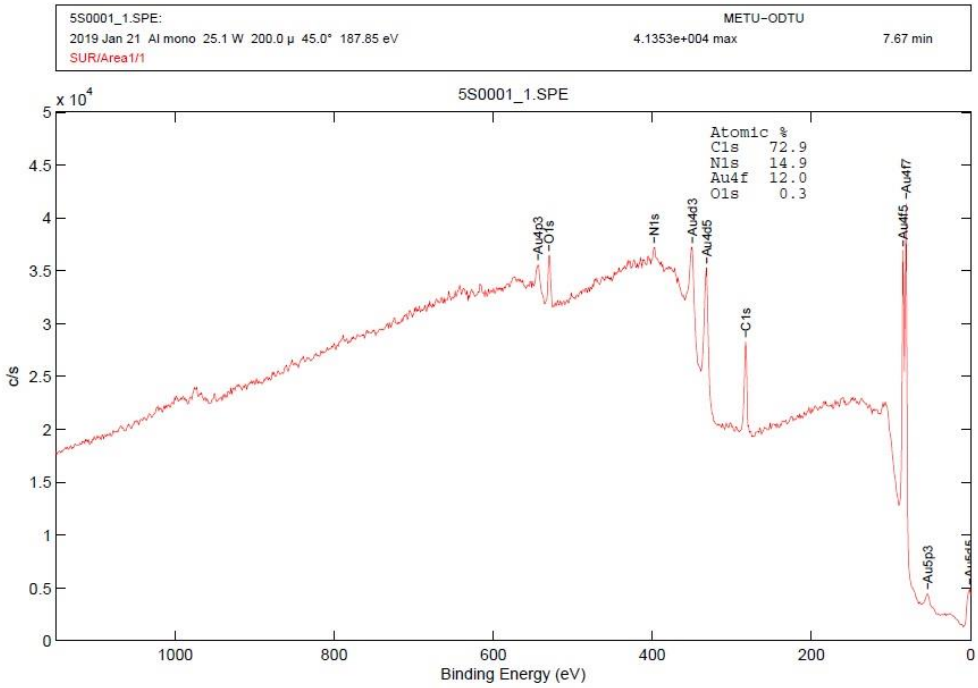

Figure S.10 XPS analysis for biotinylated antibody covered HS-PEG-COOH surface

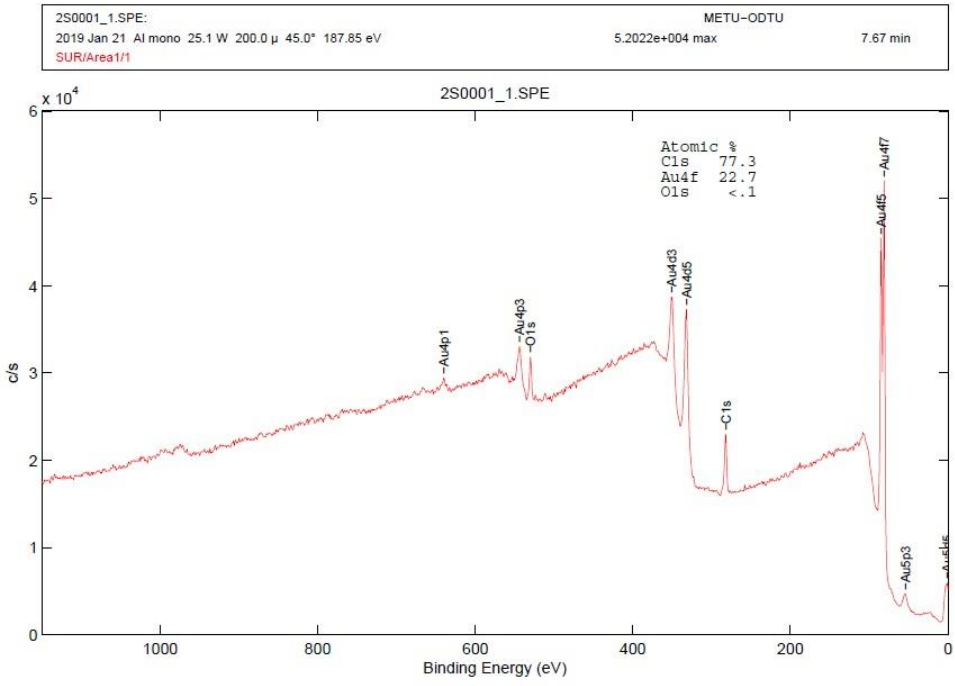

Figure S.11 XPS analysis for HS-PEG-MIX surface

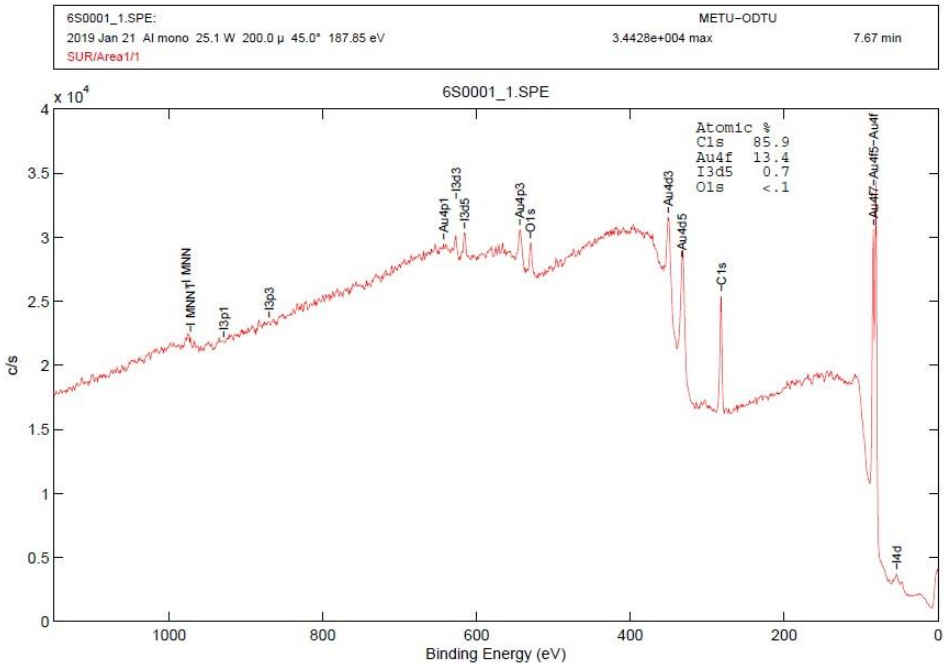

Figure S.12 XPS analysis for antibody covered HS-PEG-MIX surface

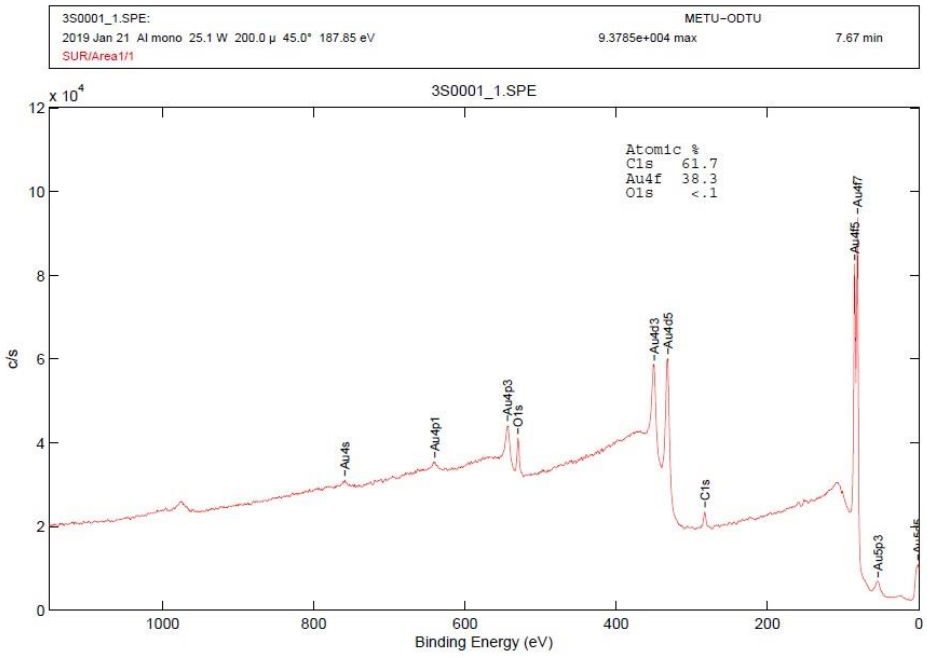

Figure S.13 XPS analysis of HS-PEG-NH2 surface

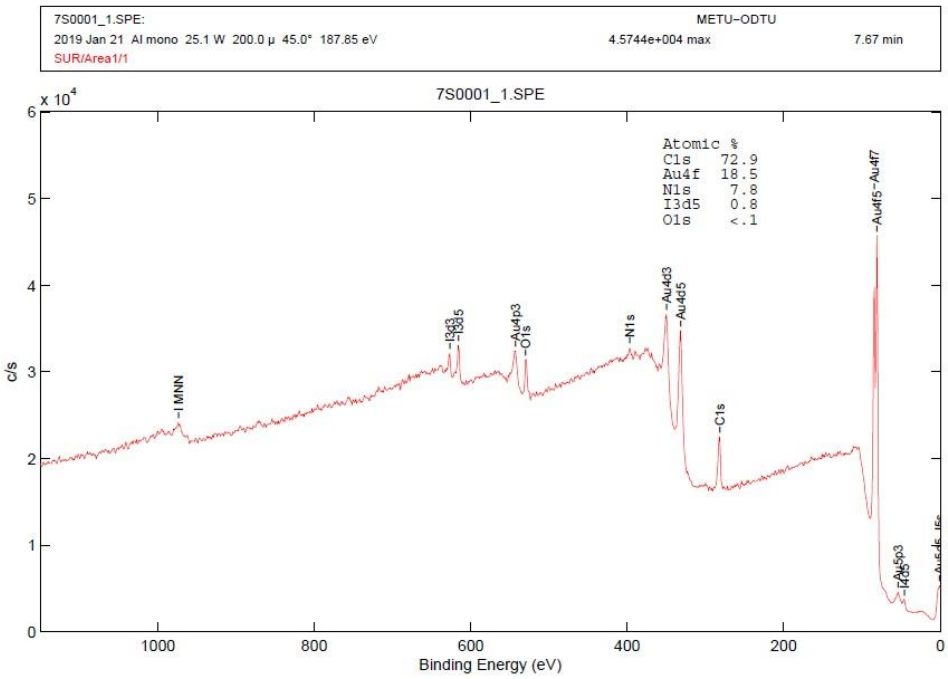

Figure S.14 XPS analysis for antibody covered HS-PEG-NH2 surface